Supplementary Information (SI) for Materials Chemistry Frontiers.

Nonpolar Graphene Oxide (GO-NP): A Heterogeneous Liquid Crystalline Alignment Medium for Anisotropic NMR in Nonpolar Organic Solvents

Sandesh Chickmagalur Jatheendranath,[a,b,c,d] Sudhindra H Deshpande,[d] and Udaya Kiran Marelli*[a,b,c]

1. Contents

1. Preparation of GO

The process for producing GO using a modified Hummer's method with water-enhanced oxidation was carried out as follows.

2 gms of graphite powder was added to 90 mL of conc. H_2SO_4 and 12 mL of water in a round-bottom flask. The mixture was placed in an ice bath and stirred for 30 minutes. 6 gms of $KMnO_4$ was then added gradually under cold conditions (maintaining the reaction temperature below 10 °C). The reaction mixture was heated to 60 °C and stirred for 4 hours or until the colour of the reaction mixture transitioned from green to dark brown. The reaction mixture was subsequently cooled to 10 °C in an ice bath and 400 mL of water was added slowly. The mixture was then heated to 80 °C and maintained at this temperature for 4 to 6 hours. The reaction mixture was further diluted with 600 mL of water and cooled to room temperature or lower in an ice bath. Then 10-15 mL of 30% hydrogen peroxide were added gradually and the mixture was stirred for 30 minutes. The solution was transferred to a beaker and allowed to settle. The supernatant was decanted and the brown solid GO was filtered and washed with 80:20 mixture of conc. HCl and water. The product was further neutralised through dialysis over a period of two days.

Thus, formed epoxy-rich GO was characterised by IR and XPS.

The IR spectrum showed (Figure **S1**) signals of stretching frequency C=O 1720 cm^{-1}, C-O-C 1230 cm^{-1}, C-O 1048 cm^{-1} and O-H 3600-3000 cm^{-1}. In the given IR spectrum intensities of epoxide C-O-C 1230cm^{-1} was stronger. XPS (figure **S2** showed the element C1S as 31%, oxygen as 67% and no traces of other elements).

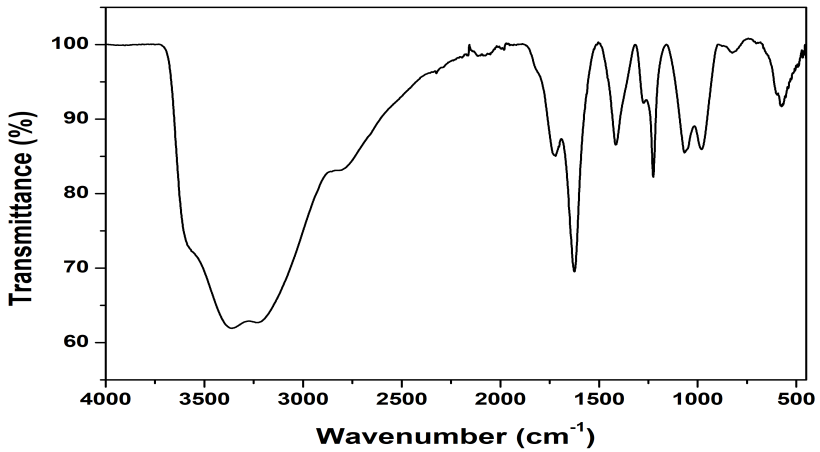

Figure S1 - IR spectrum of GO.

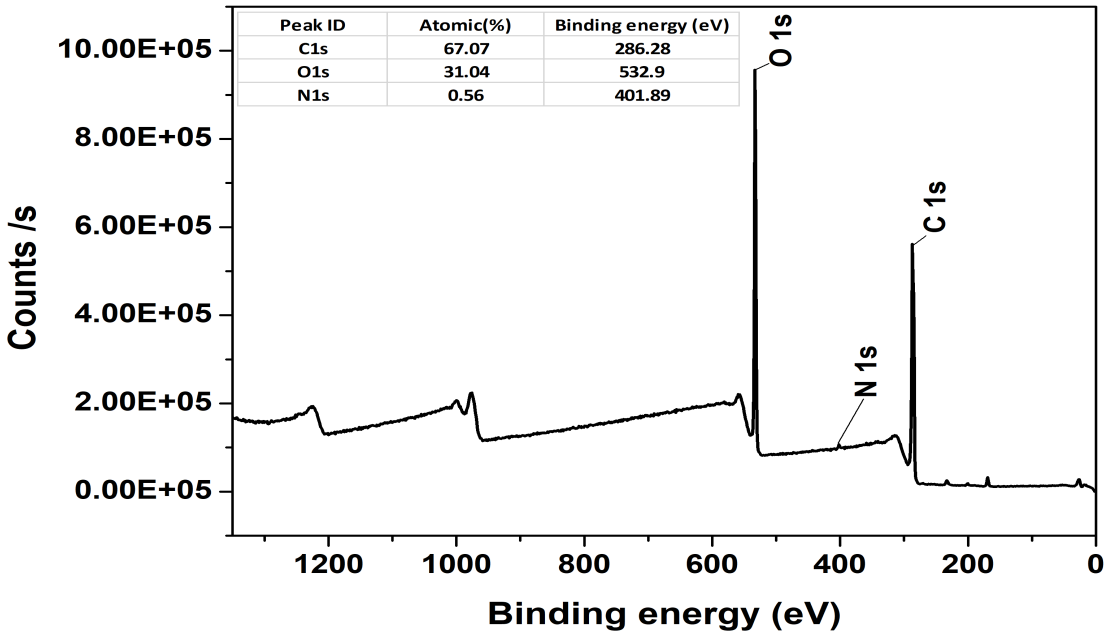

Figure S2 - XPS spectrum of GO.

2. Preparation of nonpolar GO (GO-NP)

A dispersion was prepared by sonicating 200 mg of GO in a solution of 200 mL maintaining an 80:20 volume ratio of ethanol and acetonitrile and 2 mL of amino decane were introduced. The solution was sonicated for a duration of 15 minutes in a water bath working at a frequency of 33.3 KHz. The resultant solution was subjected to centrifugation at 10,000 rpm for a period of 60 minutes to facilitate the separation of the solid phase, which was characterised by IR (Figure **S3**). The GO amino decane which is intermediate in the reaction has dispersion in intermediate polar solvent such as THF and dioxane, facilitates to perform the reaction such acid amine coupling. The isolated solid was subsequently redispersed in a 50:50 blend of tetrahydrofuran (THF) and dioxane. To this solution, 20 mL of pyridine, 1 gram of dicyclohexylcarbodiimide (DCC), 10 mg of 4-dimethylaminopyridine (DMAP), and 1 gram of stearyl amine were added, and the mixture was stirred at 90 °C overnight. The subsequent day, the reaction mixture was filtered through a Buchner funnel with filter paper and washed with acetonitrile. The final solid product was characterised using IR and XPS (Figure **S4**).

Infrared (IR) and X-ray photoelectron spectroscopy (XPS) was used to analyse the chemical composition of the GO-NP sample. The IR data revealed stretching frequencies in the sample including the CH stretching (alkane) stretching at 2850 and 2951 cm^{-1} and broad OH and NH

peaks in the range of 3600-3000 cm^{-1}. The XPS analysis of the GO-NP sample showed an elemental composition of 77% carbon 15% oxygen and 6% nitrogen.

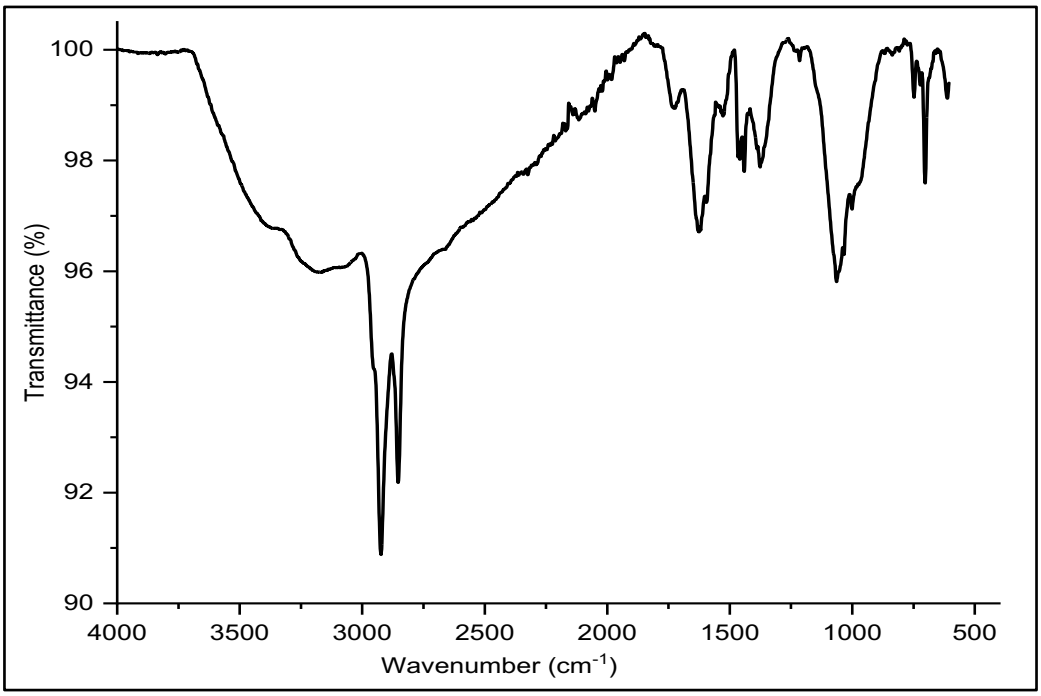

Figure S3 - IR spectrum of GO-amino decane. The stretching frequencies of 2850-2960 cm^{-1} indicates the presence of alkane on surface of GO.

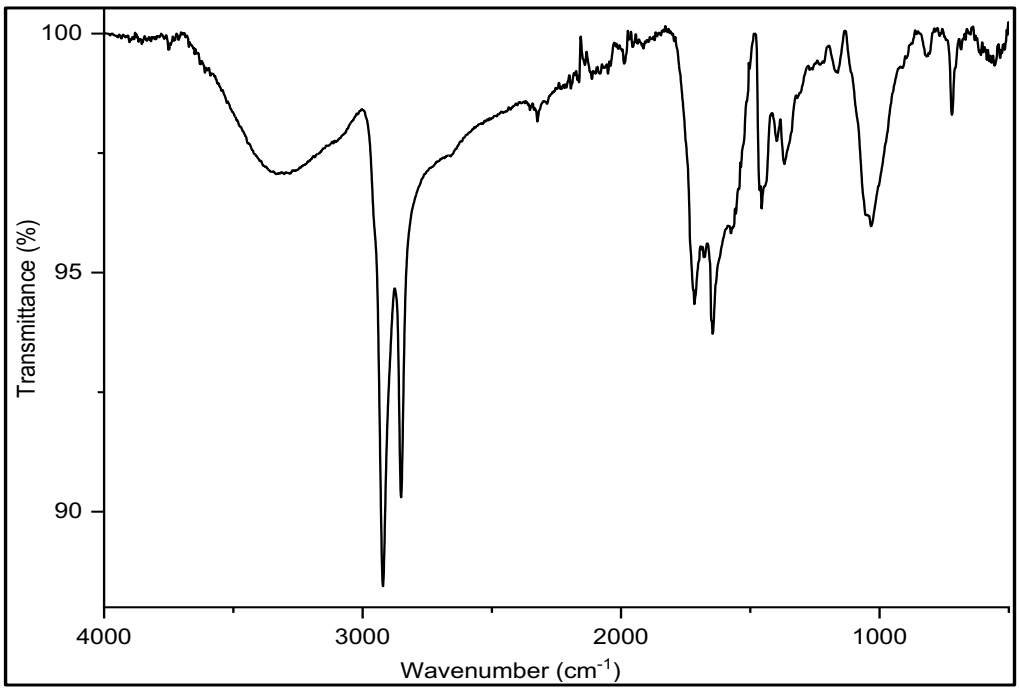

Figure S4 - IR spectrum of GO-NP.

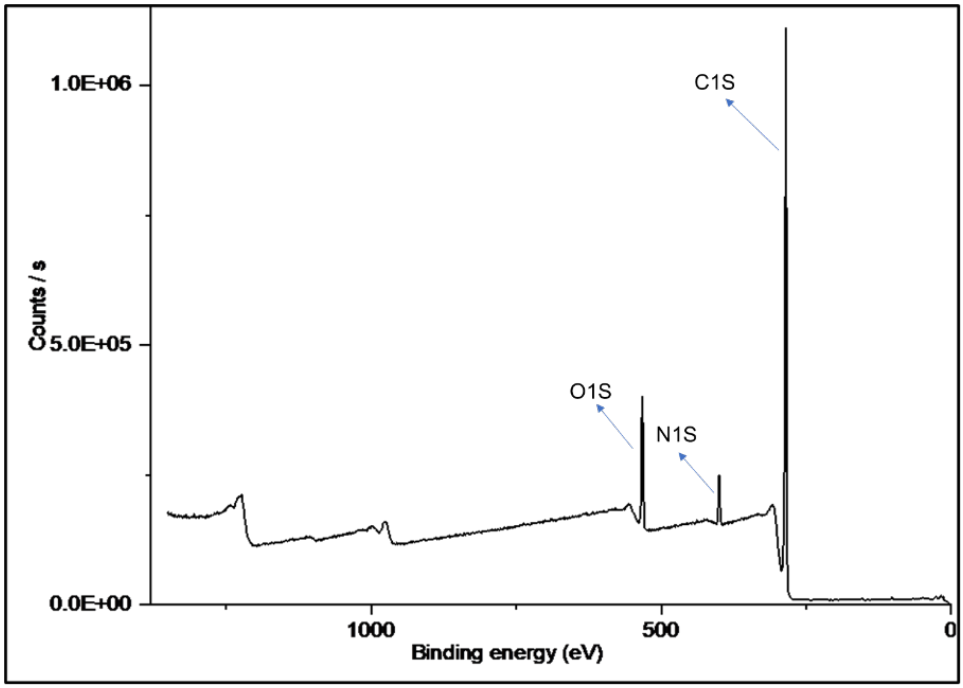

Figure S5 - XPS spectrum of GO-NP.

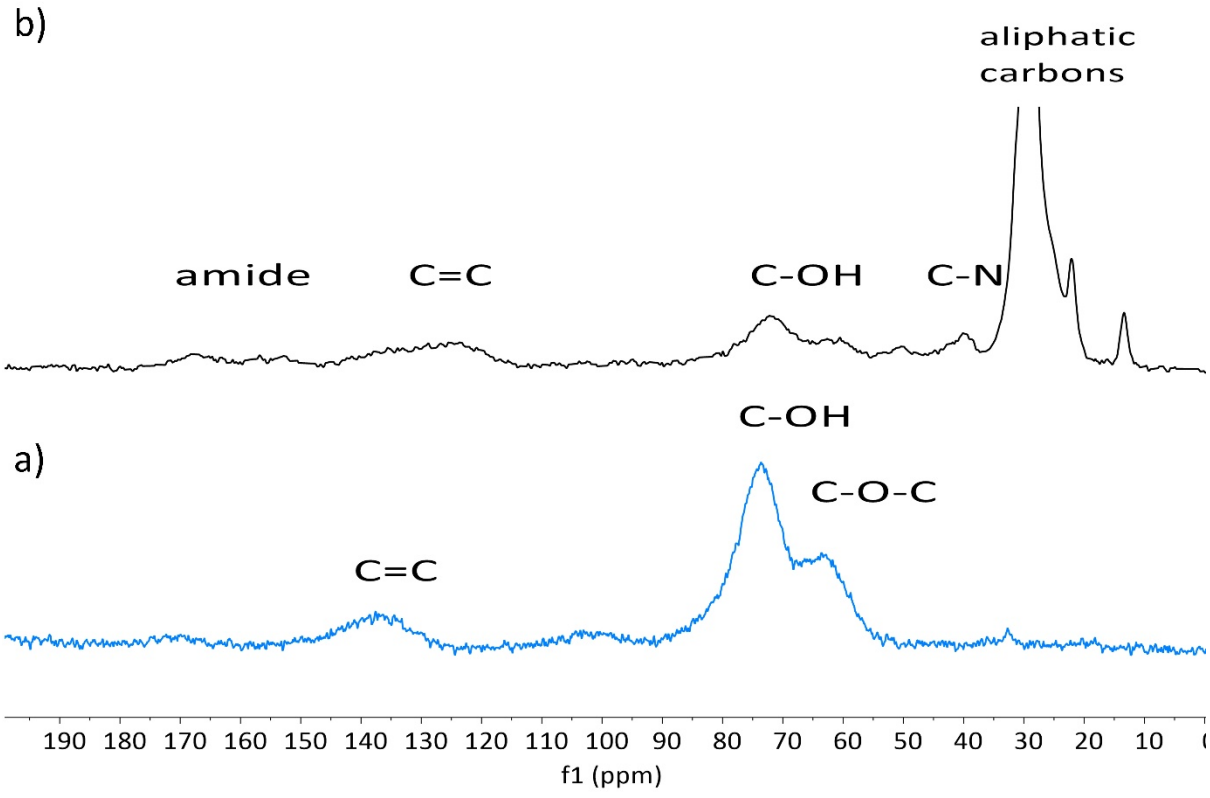

Figure S6 : Overlay of the solid-state ^{13}C-CPMAS spectra of (a) epoxy-rich GO and (b) GO-NP NMR showing the differences in the chemical shift resonances between the two. Epoxy-rich GO showed C-O-C resonance at 65 ppm, C-OH resonance at 74 ppm and C=C graphite resonance at ~120-150 ppm. GO-NP showed aliphatic ^{13}C shifts from aliphatic alkyl amines at ~23-30 ppm, C-N resonances from alkyl amine at 39.8 ppm and amide carbonyl at 168.0 ppm. A strong resonance in GO-NP at ~23-30 ppm along with the other C-N resonances, support the derivatisation of epoxy-rich GO by aliphatic alkyl amines and thus its conversion to GO-NP. The solid-state ^{13}C-CPMAS experiments were

carried out on a Bruker 500 MHz AVANCE NEO spectrometer at a ^{13}C frequency of 125.86 MHz, using a magic-angle spinning (MAS) rate of 10,000 Hz in both cases.

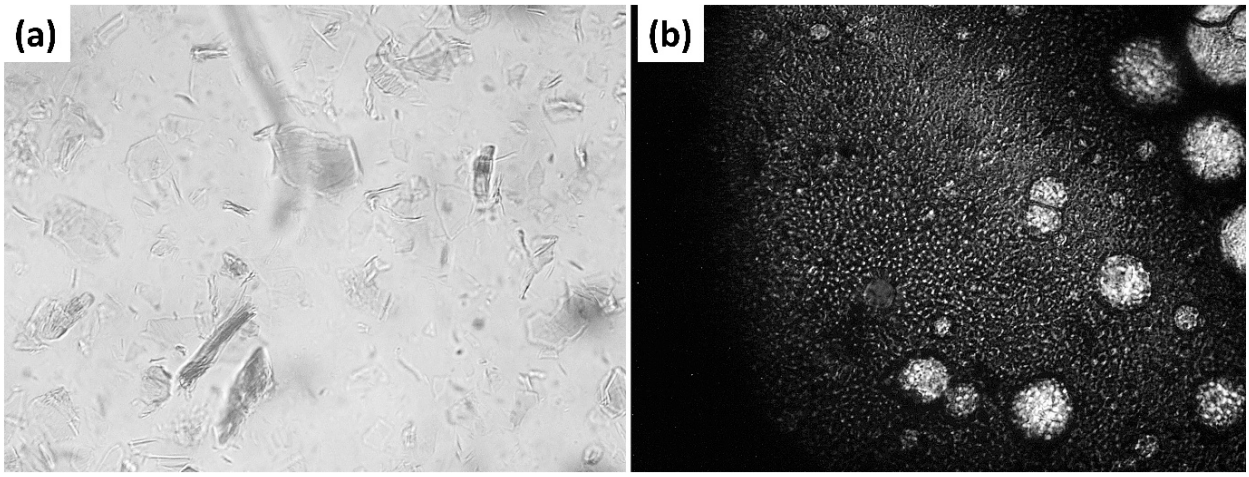

Figure S7: Polarised optical microscopy (POM) images of (a) epoxy-rich GO (15 mg/mL) in ethanol demonstrating complete dispersion after sonication, but no visible crystalline pattern; (b) GO-NP (15.5 mg/mL) in DCM exhibiting partially ordered LC after sonication. To clarify further, the POM for GO-NP in DCM cannot be recorded, as it forms partial aggregates and precipitates. All polarised optical spectroscopy images were recorded using a Magnus MLXI-TR Plus LED trinocular microscope (Magnus Opto Systems, India) equipped with crossed polarisers. The microscope was fitted with an LED illumination source, and images were captured through the trinocular port using a digital camera attachment. All measurements were performed under ambient laboratory conditions.

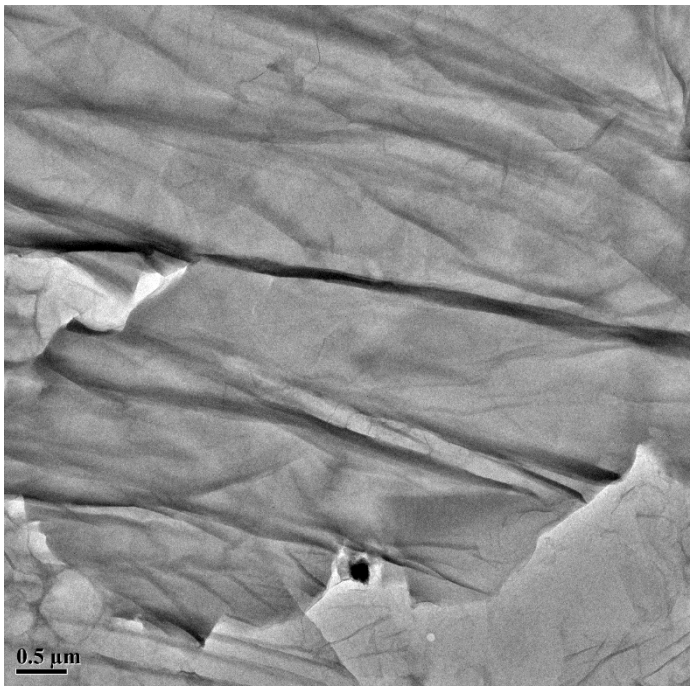

Figure S8: The TEM image of the epoxy-rich GO shows dense, highly stacked plate-like structures with strong mass-thickness contrast. The particles appear as compact, multilayered graphitic domains with relatively smooth and rigid morphology. Individual sheets are not clearly distinguishable due to tight interlayer π–π stacking. The structures exhibit low electron transparency, indicating significant thickness. Lateral

dimensions are in the sub-micrometre to micrometre range, but the vertical thickness is high, giving low aspect ratio (lateral size/thickness) platelets characteristic of bulk layered graphite-like materials.

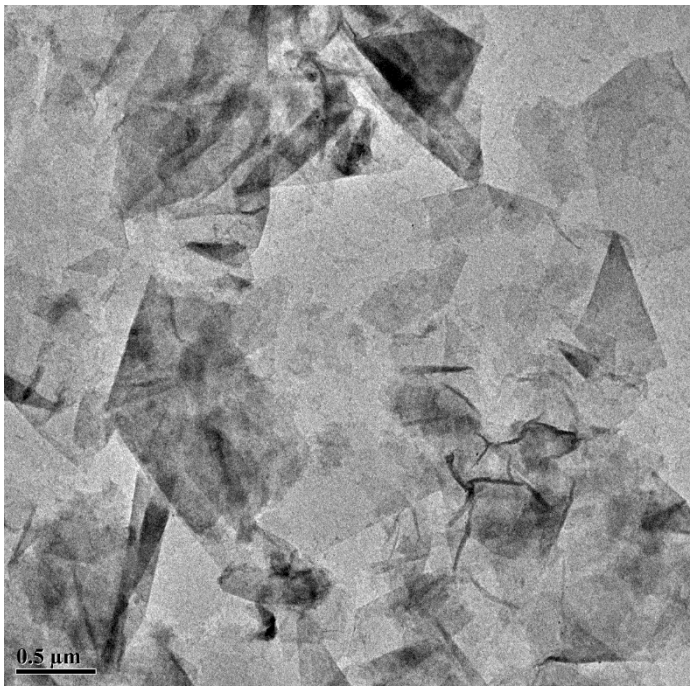

Figure S9. Transmission electron microscopy (TEM) image of GO-NP illustrating ultrathin, electron-transparent nanosheets with lateral sizes in the range of ~0.3–1.5 µm. The presence of wrinkles, corrugations, and folded edges confirms the flexible few-layer structure, while darker contrast regions correspond to overlapping sheets and partial restacking.

In contrast to epoxy-rich GO, the derivatised GO–NP sample displays thin, electron-transparent nanosheets with pronounced wrinkles, folds, and corrugations, indicating ultrathin and mechanically flexible layers. The sheets are well exfoliated and exhibit paper-like morphology with lateral dimensions of approximately 0.3–1.5 µm. Darker regions correspond to local overlap or partial restacking, but most areas show reduced contrast consistent with few-layer structures. The presence of surface undulations further confirms decreased thickness and enhanced flexibility following oxidation and derivatisation.

3. NMR experiments details

NMR spectra were recorded using a Bruker Spectrometer operating at 500.13 MHz for ^{1}H and 125.76 MHz for ^{13}C with all spectra being measured at 25 °C in a 5-mm NMR tube using DMSO-d_6 (D 99.9%) as a solvent. ^{2}H NMR spectra were acquired to measure the quadrupolar coupling of the solvent by measuring signal splitting and evaluating the degree of alignment and homogeneity of the medium.[1] F2-coupled *[$^{1}H^{13}C$]* CLIP-HSQC experiments were carried out using 16-32 scans a relaxation delay of 2-3 s 256 (t1) × 4026 (t2) real data point The NMR spectra were recorded for both the isotropic sample (*$CDCl_3$*) and the GO-NP.

To demonstrate the alignment properties of the GO-NP LCs we carried out RDC measurements for all chosen molecules. To acquire the RDCs *J*-resolved [$^{1}H^{13}C$] CLIP-HSQC spectra were recorded under both alignment conditions. $^{1}D_{C\text{-}H}$ RDCs were extracted by subtracting the coupling observed under the minimum alignment conditions $^{1}J_{CH}$ from the coupling observed under the maximum alignment conditions $^{1}T_{CH}$, Using equation (1.1).

$$^{1}T_{CH} = {}^{1}J_{CH} + {}^{1}D_{CH} \quad (1.1)$$

4. DFT calculations for RDC

Computed RDCs were obtained using two steps: conformer generation by molecular mechanics and geometry optimisation

All four molecules—santonin, menthol, artemisinin, and strychnine—exhibit moderate flexibility. For each molecule, possible diastereomers were identified, and conformers for each diastereomer were generated using the macromodel conformer search program (Schrödinger) with an energy constraint of 20 kcal mol^{-1}.[1,2]

The obtained conformers were refined under geometry optimisation job using Schrödinger maestro material science package employing DFT with B3LYP/631+G(dp) theory. [3,4]

5. NMR data and structural calculations of santonin

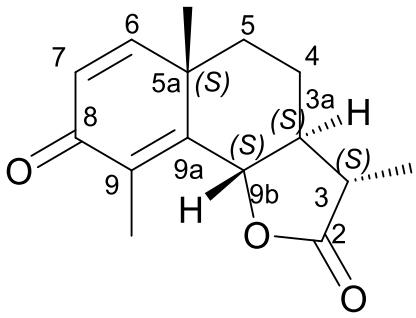

Figure S10 - Structure of santonin.

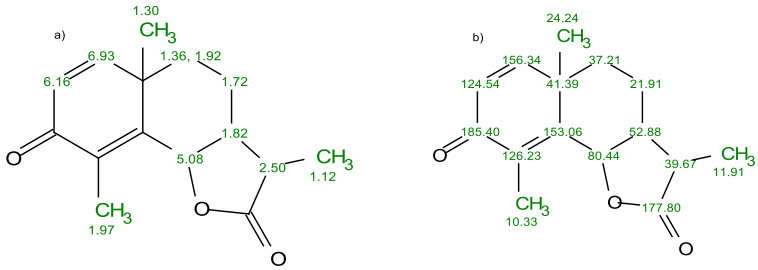

Figure S11 - (a) ^{1}H and (b) ^{13}C chemical shift assignment.

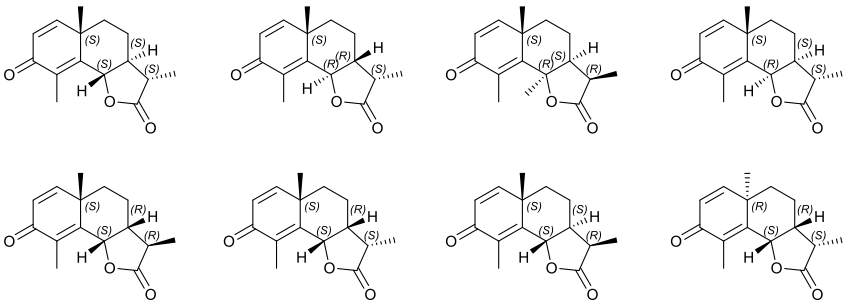

Figure S12- structures of possible diastereomers of santonin.

Atom numbers		
Stru Number	DFT Number	^{13}C chemical shift assignment (ppm)
C8	12	185.5
C2	3	177.9
C6	14	156.5
C9a	10	153.1
C9	11	126.2
C7	13	124.6
C9b	5	80.5
C3a	6	52.9
C5a	9	41.4
C3	1	39.8
C5	8	37.3
C5a-Me	17	24.5
C4	7	21.9
C3-Me	1	12.1
C9-Me	16	10.6

Table S1 - Atom numbers and ^{13}C chemical shift assignment of santonin.

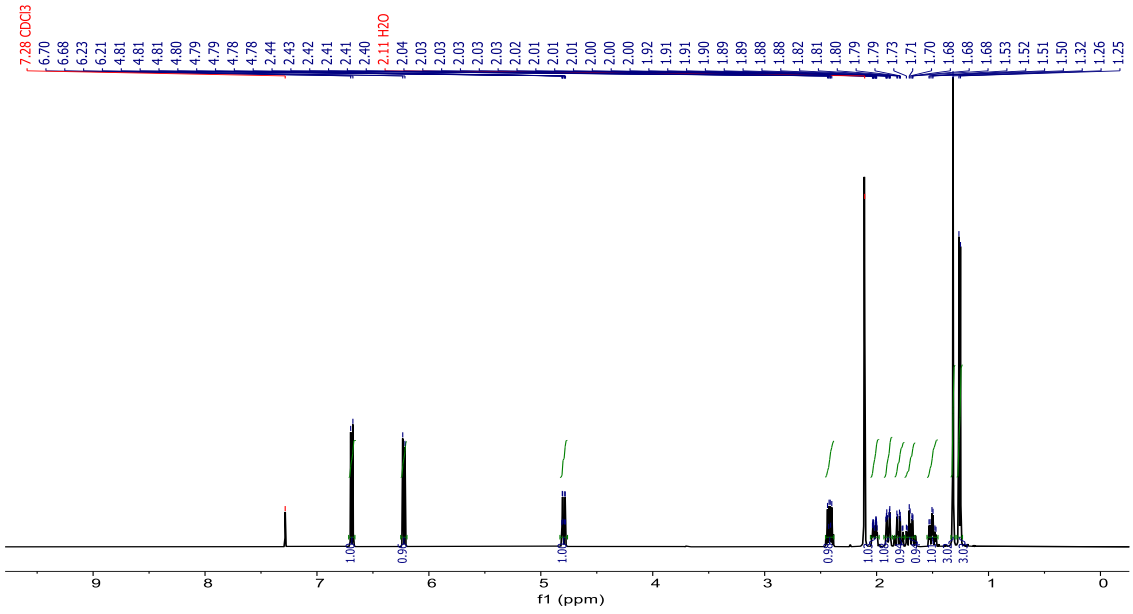

Figure S13 - ^{1}H NMR (500 MHz) of santonin in $CDCl_3$ at 298 K.

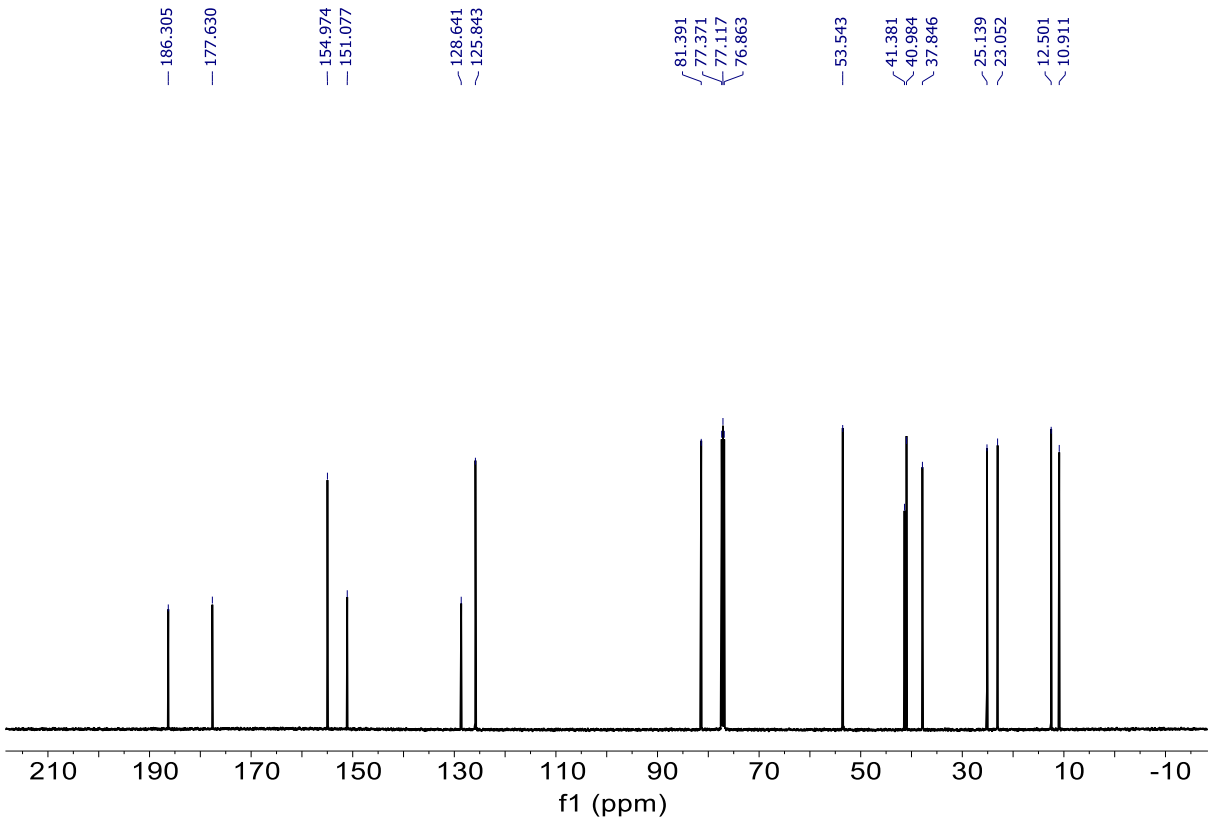

Figure S14 - ^{13}C NMR (125 MHz) of santonin in $CDCl_3$ at 298 K.

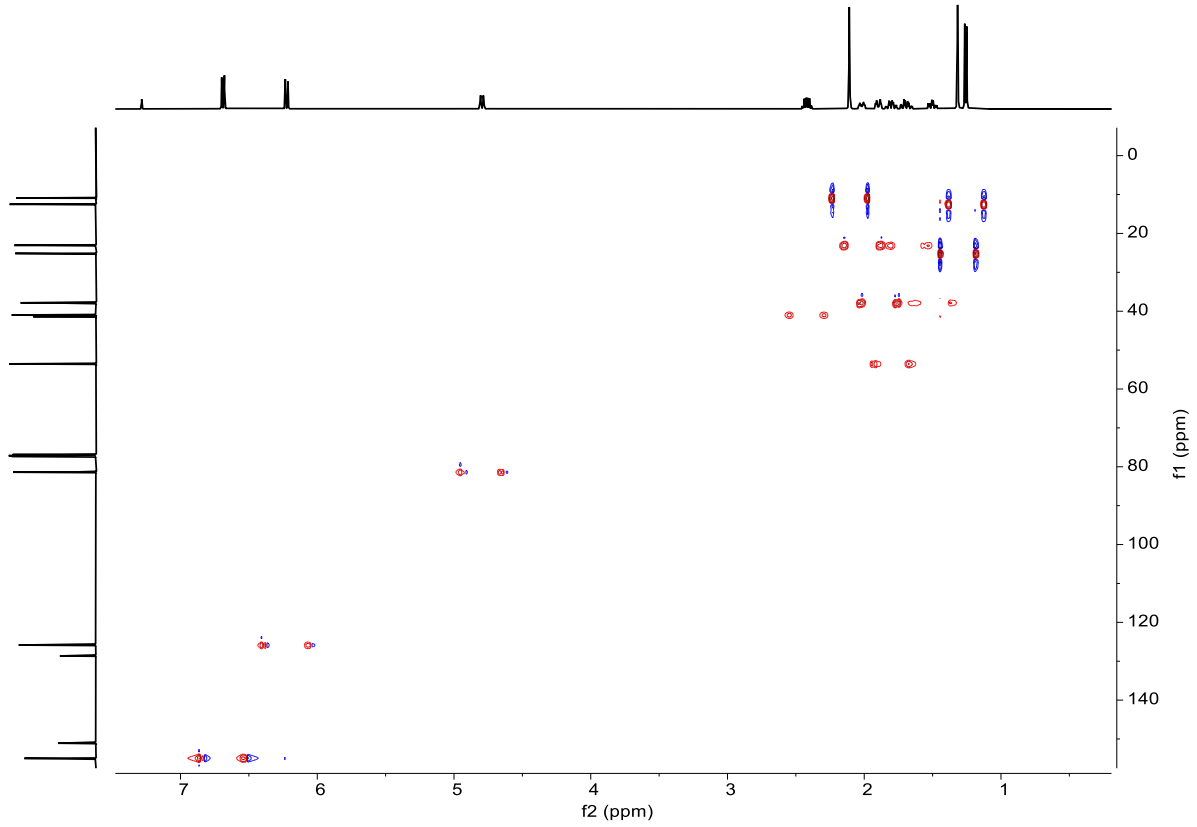

Figure S15 - [$^{1}H^{13}C$] CLIP-HSQC (500 MHz) of santonin in $CDCl_3$ at 298 K.

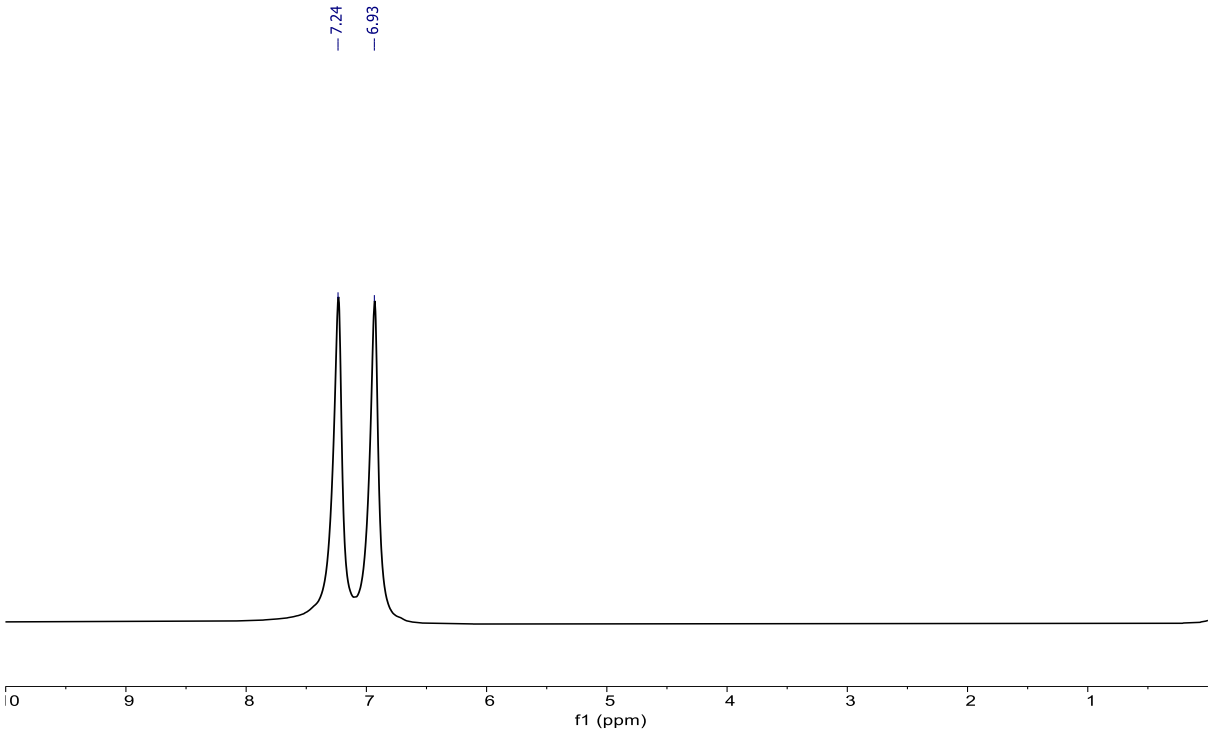

Figure S16 – ^{2}H NMR (75.6 MHz) of 9.74 mg/mL santonin and 18.5 mg/mL of GO-NP in $CDCl_3$ at 298 K after sonication.

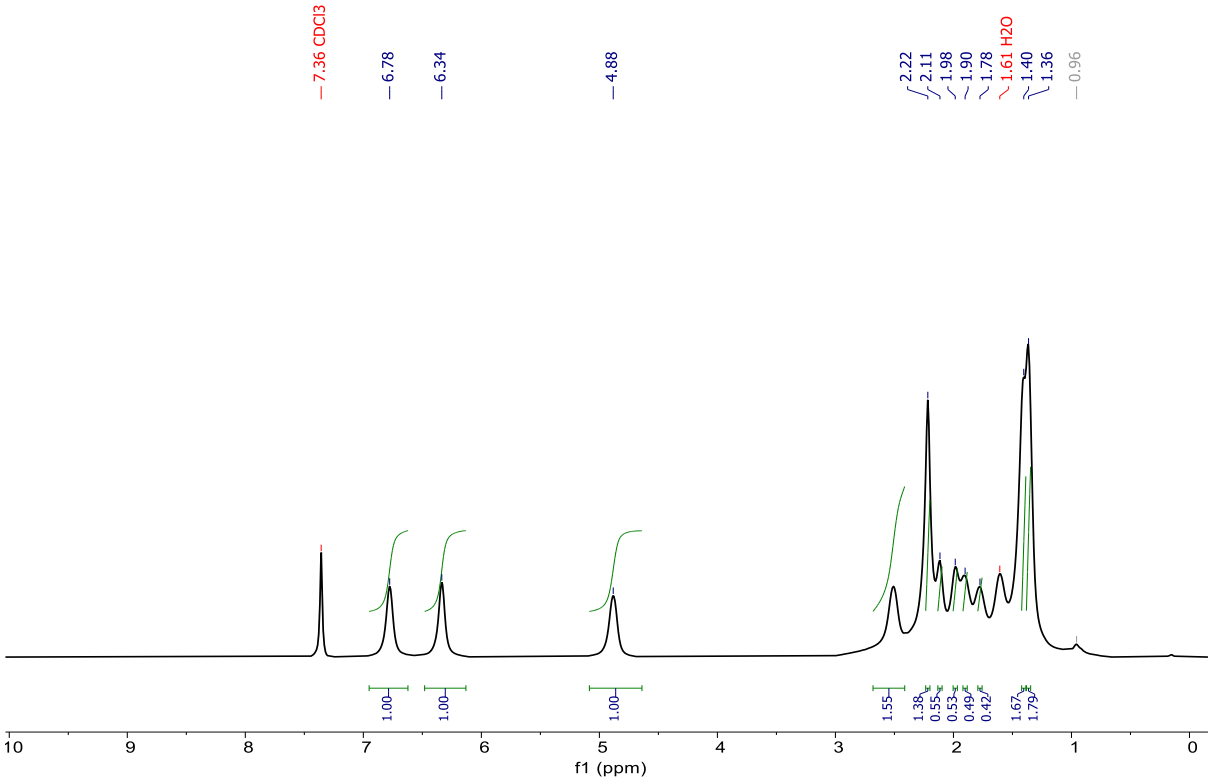

Figure S17 - ^{1}H NMR (500 MHz) of 9.74 mg/mL santonin and 18.5 mg/mL of GO-NP in $CDCl_3$ at 298 K after sonication.

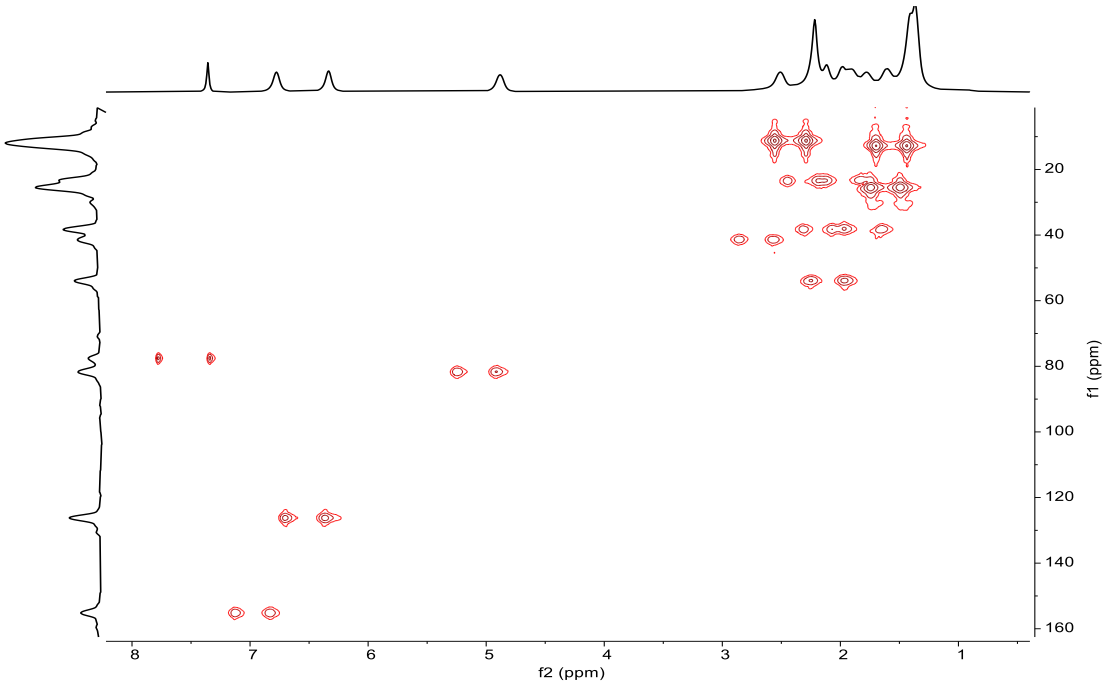

Figure S18 - [$^{1}H^{13}C$] CLIP-HSQC of 9.74 mg/mL santonin and 18.5 mg/mL of GO-NP in $CDCl_3$ at 298 K after sonication.

5.1. RDC of santonin

diastereomer *SSSS*		
Q = 0.13		
	Exp Hz	Comp Hz
C14,H30	-6.94	-7.11
C13,H29	9.01	8.84
C5,H23	2.94	6.99
C6,H24	17.91	13.74
C2,H22	14.3	13.95
C8,H28	-5.22	-5.26
C8,H27	30.63	31.35
C17,H34	0.18	2.75
C17,H35	0.18	2.75
C17,H36	0.18	2.75
C7,H25	12.52	12.74
C7,H26	36.29	36.26
C16,H31	2.5	4.07
C16,H32	2.5	4.07
C16,H33	2.5	4.07
C1,H20	3.17	6.41
C1,H19	3.17	6.41
C1,H21	3.17	6.41

Table S2 - Atom numbers and RDC values (experimental and calculated) for the SSSS diastereomer of santonin.

5.2. SVD fitting of the santonin

Conformer 1

Alignment tensor

A'x=-2.429e-04

A'y=-5.390e-04

A'z= 7.819e-04

Saupe tensor

S'x=-3.643e-04

S'y=-8.085e-04

S'z= 1.173e-03

Alignment tensor eigenvectors

e[x]=(0.177, 0.346, 0.921)

e[y]=(-0.302,-0.872, 0.385)

e[z]=(0.937,-0.346,-0.050)

Alignment tensor in laboratory coordinates:

[6.294e-04,-4.106e-04,-1.311e-05]

[-4.106e-04,-3.450e-04,1.171e-04]

[-1.311e-05,1.171e-04,-2.844e-04]

SVD condition number is 4.122e+00

Axial component Aa = 1.173e-03

Rhombic component Ar = 2.961e-04

rhombicity R = 0.252

Asimmetry parameter etha =3.787e-01

GDO = 1.402e-03

Euler Angles (degrees)

Set 1

(-98.1,-69.5,-59.7)

Set 2

(81.9,249.5,120.3)

Grid points: 64

Diastereomers	RDC (*Q*)
SSSS	0.096
SSSR	0.466
RRSR	0.555
SRSS	0.417
RRSS	0.778
RSSR	0.61
SRSR	0.436
RSSS	0.744

Table S3 - Q factors derived from RDC calculations for all diastereomers of santonin.

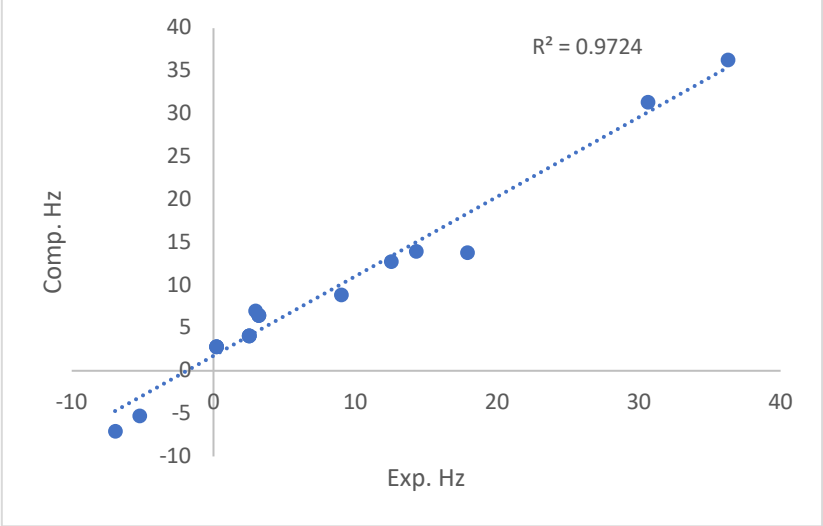

Figure S19 - Plot showing experimental versus calculated RDCs for the SSSS diastereomer of santonin.

6. NMR data and structural calculations of menthol.

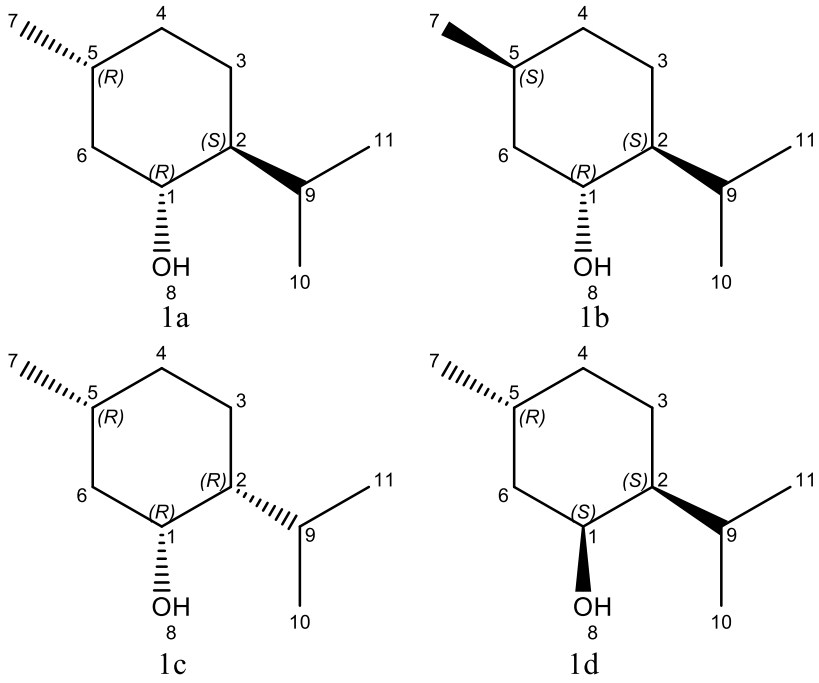

Figure S20 - Structures of all possible diastereomers of menthol.

Atom numbers		
Using chemdraw numbering	DFT atom number	^{13}C chemical shift assignment (ppm)
7	1	16.11
10	7	21.06
11	8	22.2
4	3	23.2
4	3	23.2
9	6	25.9
5	2	31.7
3	4	34.6
3	4	34.6
6	11	45.05
6	11	45.05
2	5	50.18
1	9	71.58

Table S4 - Atom numbers and 13C chemical shift assignments of menthol in $CDCl_3$.

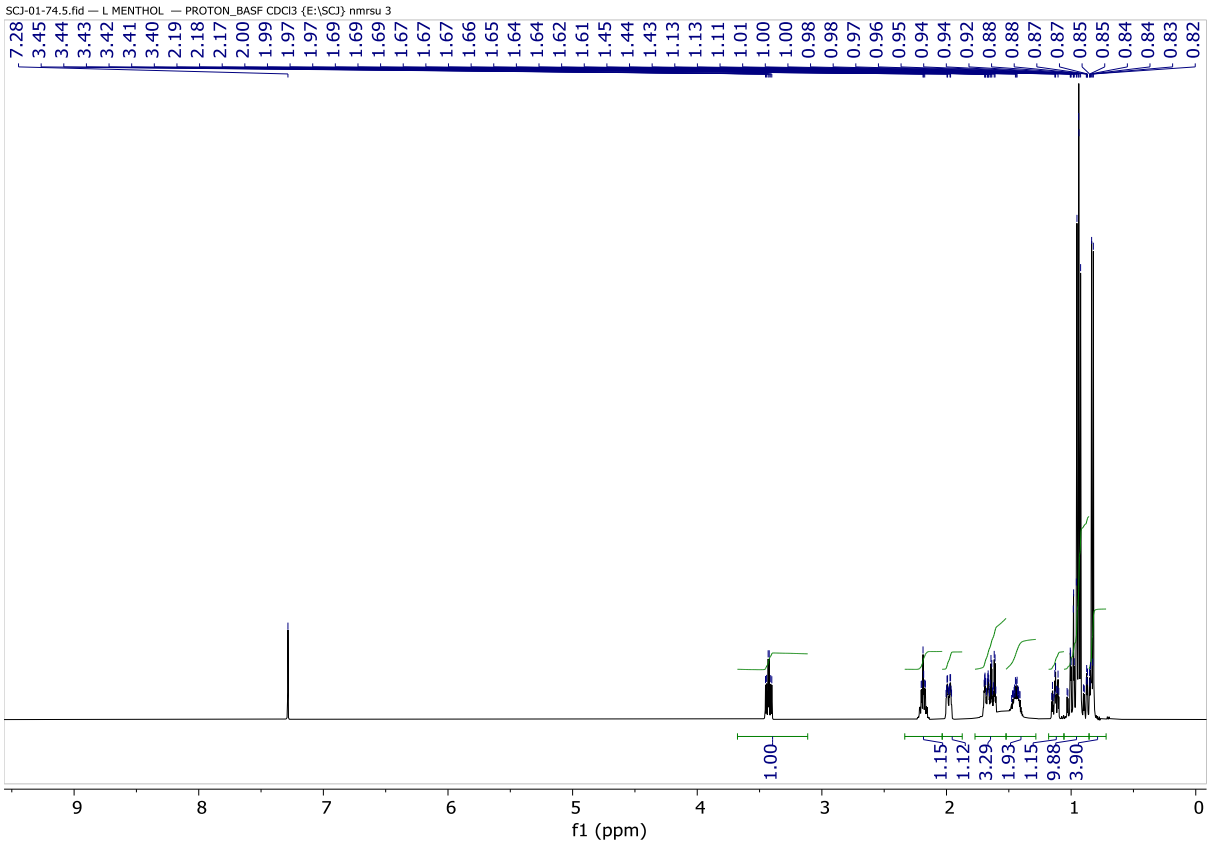

Figure S21 - ^{1}H NMR (500 MHz) of menthol in $CDCl_3$ at 298 K.

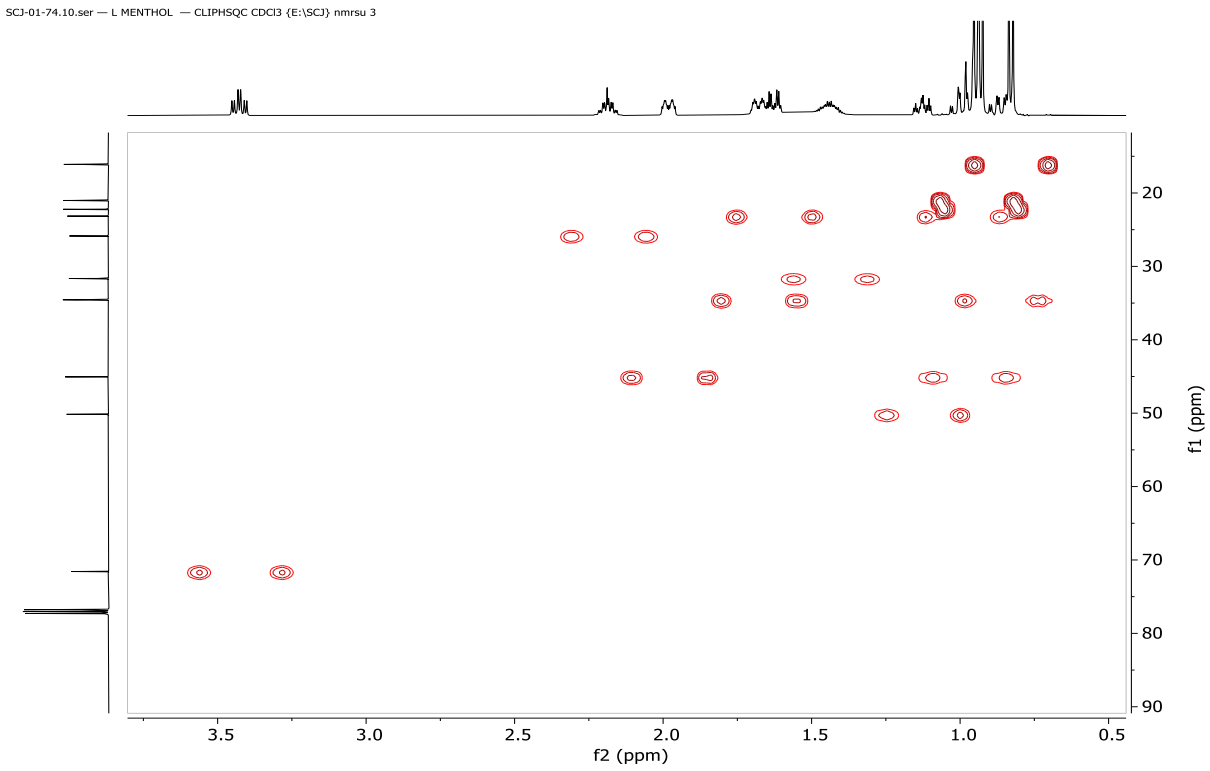

Figure S22 - $[^{1}H^{13}C]$-CLIP-HSQC (500 MHz) of menthol in $CDCl_3$ at 298 K.

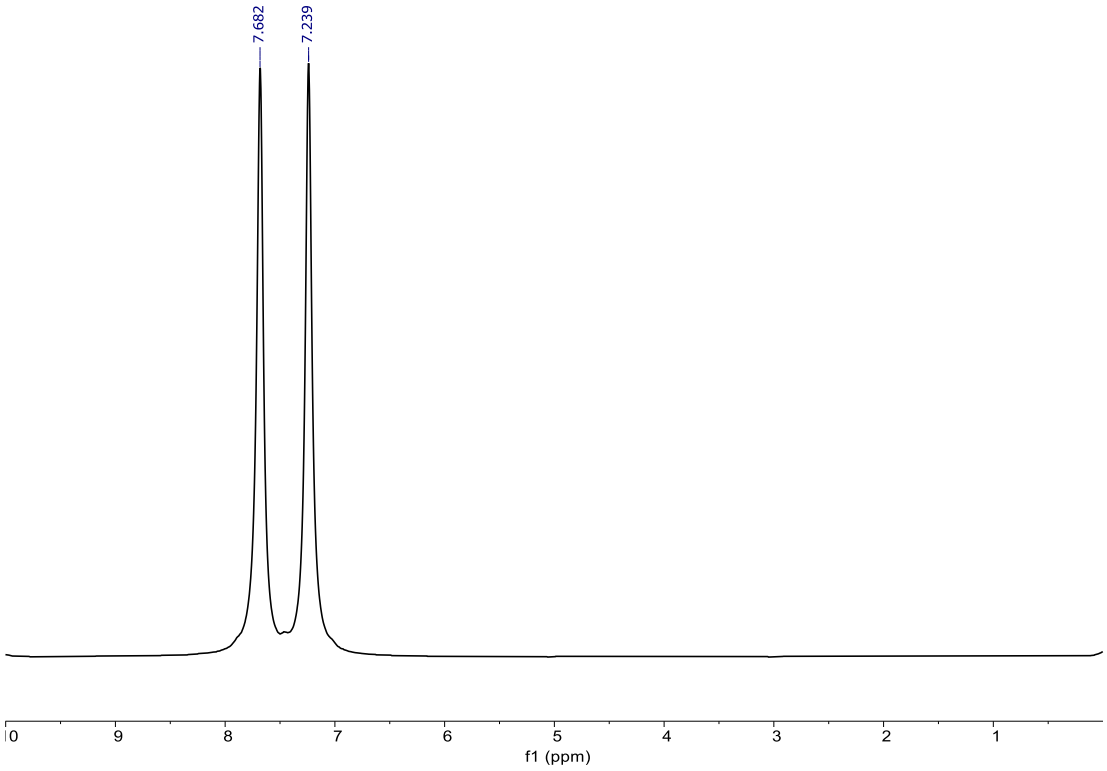

Figure S23 - ^{2}H NMR (75.6 MHz) of 15.7 mg/mL menthol and 18.1 mg/mL of GO-NP in $CDCl_3$ at 298 K after sonication.

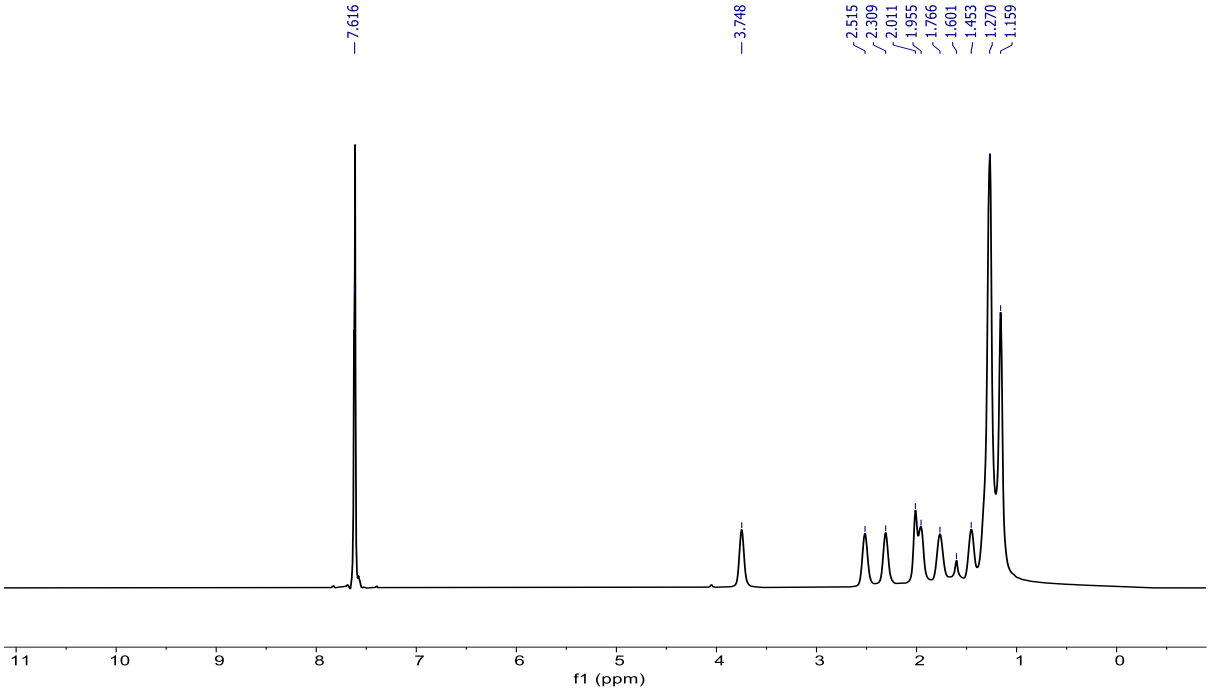

Figure S24 - ^{1}H NMR (500 MHz) of 15.7 mg/mL menthol and 18.1 mg/mL of GO-NP in $CDCl_3$ at 298 K after sonication.

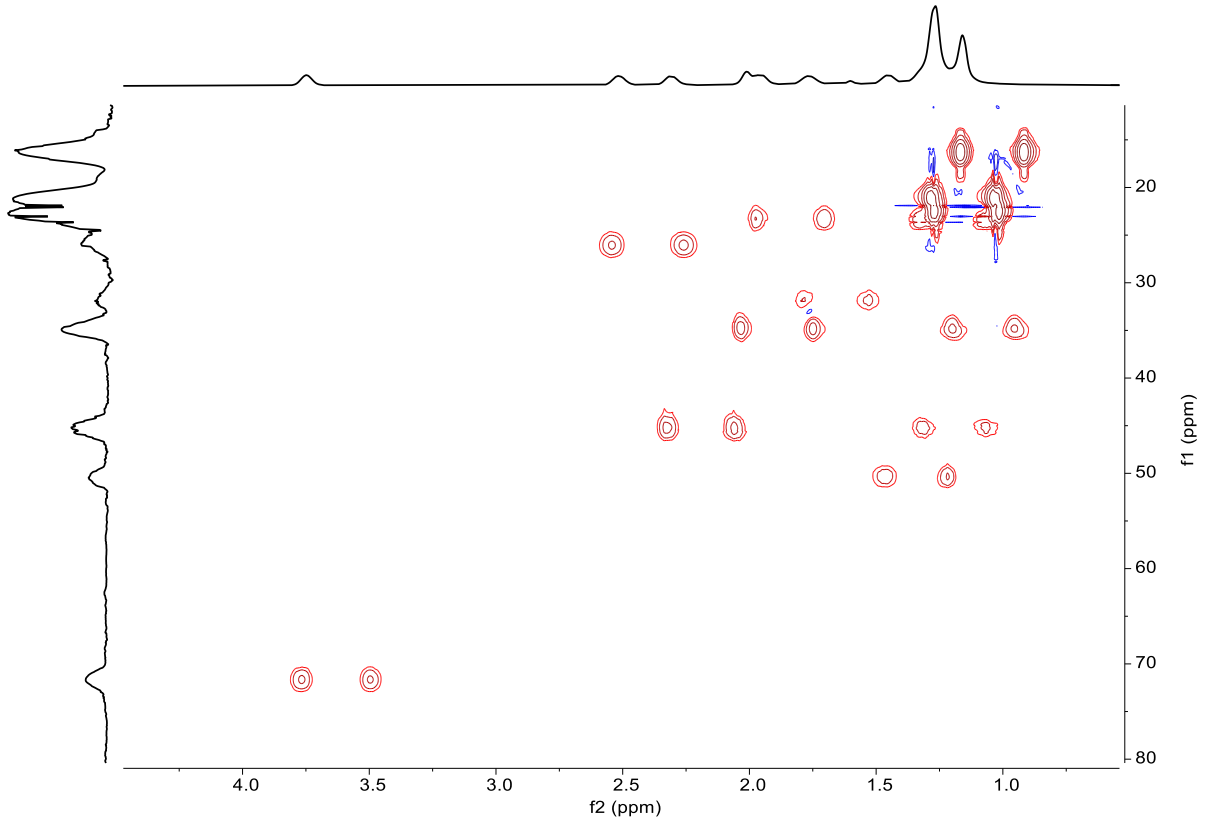

Figure S25 - [$^{1}H^{13}C$] CLIP-HSQC of 15.7 mg/mL menthol and 18.1 mg/mL of GO-NP in $CDCl_3$ at 298 K after sonication.

6.1. RDC of menthol

diastereomer *RSR*		
Q = 0.018		
	Exp Hz	Comp Hz
C4,H18	6.9	6.57
C4,H19	0.42	0.33
C6,H21	17.78	17.77
C2,H15	5.69	5.68
C3,H16	16.57	16.6
C3,H17	0.86	0.87
C11,H30	5.15	5.48
C11,H31	1.22	1.3

Table S5 - Atom numbers and RDC values (experimental and calculated) for the RSR diastereomer of menthol.

6.2. SVD fitting of the menthol

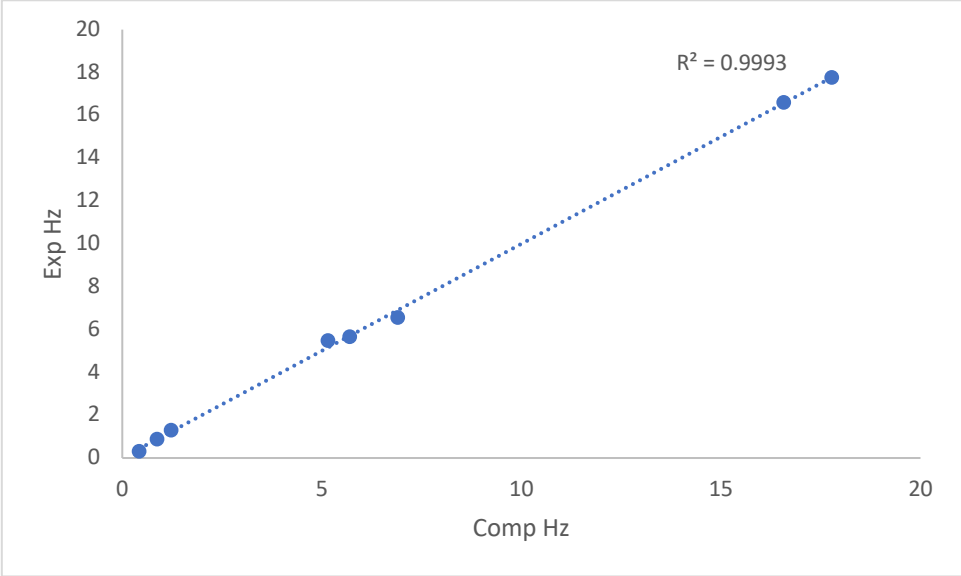

Figure S26 - Plot showing experimental versus calculated RDCs for the RSR diastereomer of menthol.

SVD parameters

Conformationally averaged solution

Alignment tensor

A'x= 5.334e-04

A'y= 9.552e-04

A'z=-1.489e-03

Saupe tensor

S'x= 8.002e-04

S'y= 1.433e-03

S'z=-2.233e-03

Alignment tensor eigenvectors

e[x]=(0.484, 0.864,-0.140)

e[y]=(0.721,-0.302, 0.623)

e[z]=(0.496,-0.403,-0.769)

Alignment tensor in laboratory coordinates:

[2.557e-04,3.117e-04,9.610e-04]

[3.117e-04,2.442e-04,-7.060e-04]

[9.610e-04,-7.060e-04,-4.998e-04]

SVD condition number is 1.254e+01

Axial component Aa = -2.233e-03

Rhombic component Ar = -4.218e-04

rhombicity R = 0.189

Asimmetry parameter etha =2.833e-01

GDO = 2.630e-03

Euler Angles (degrees)

Set 1

(-152.4,-29.7,56.2)

Set 2

(27.6,209.7,-123.8)

Grid points: 64

Diastereomers	Q
RSR	0.018
RRR	0.136
RSS	0.118
SSR	0.150

Table S6 - Atom numbers and RDC values (experimental and calculated) for all possible diastereomers of menthol.

7. NMR data and structural calculations of artemisinin

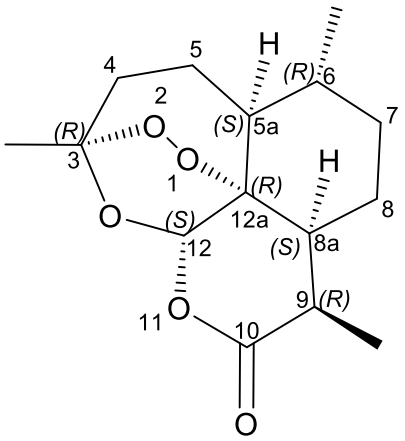

(+)-artemisinin

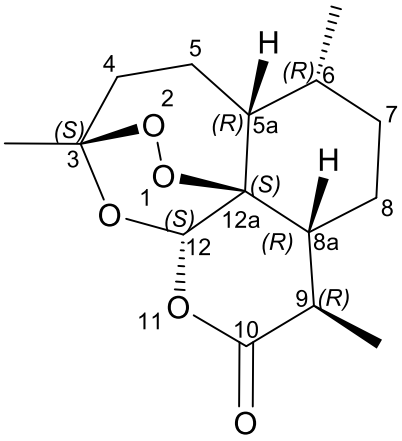

9-*epimer* artemisinin

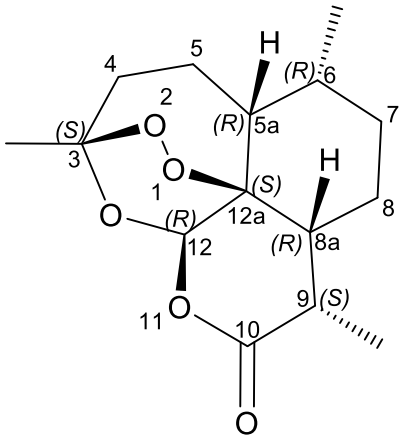

6-*epimer*-artemisinin

Figure S27 - Structure of (1) artemisinin, (2) 9-epi-artemesinin and (3) 6-epi-artemisinin.

Atom numbering		
chemdraw numbering	DFT Numbering	^{13}C chemical shift assignment (ppm)
7	C7	93.74
3	C3	50.08
8	C8	44.97
11	C11	37.52
1	C1	35.92
10	C10	33.61
14	C14	32.91
17	C21	25.21
2	C2	24.87
9	C9	23.41
20	C17	19.85
16	C16	12.98

Table S7 - Atom numbers and 13C chemical shift assignments of artemisinin in $CDCl_3$.

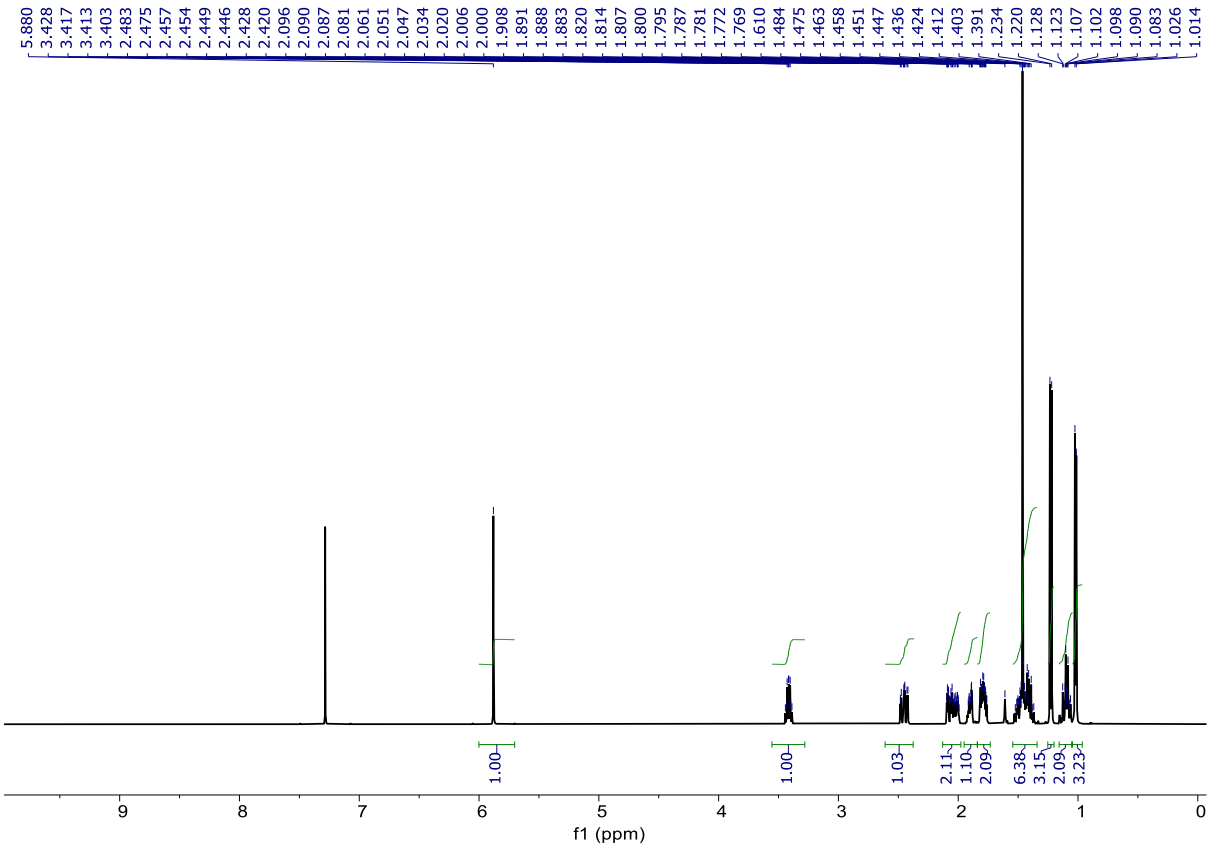

Figure S28 - ^{1}H NMR (500 MHz) of artemisinin in $CDCl_3$ at 298 K.

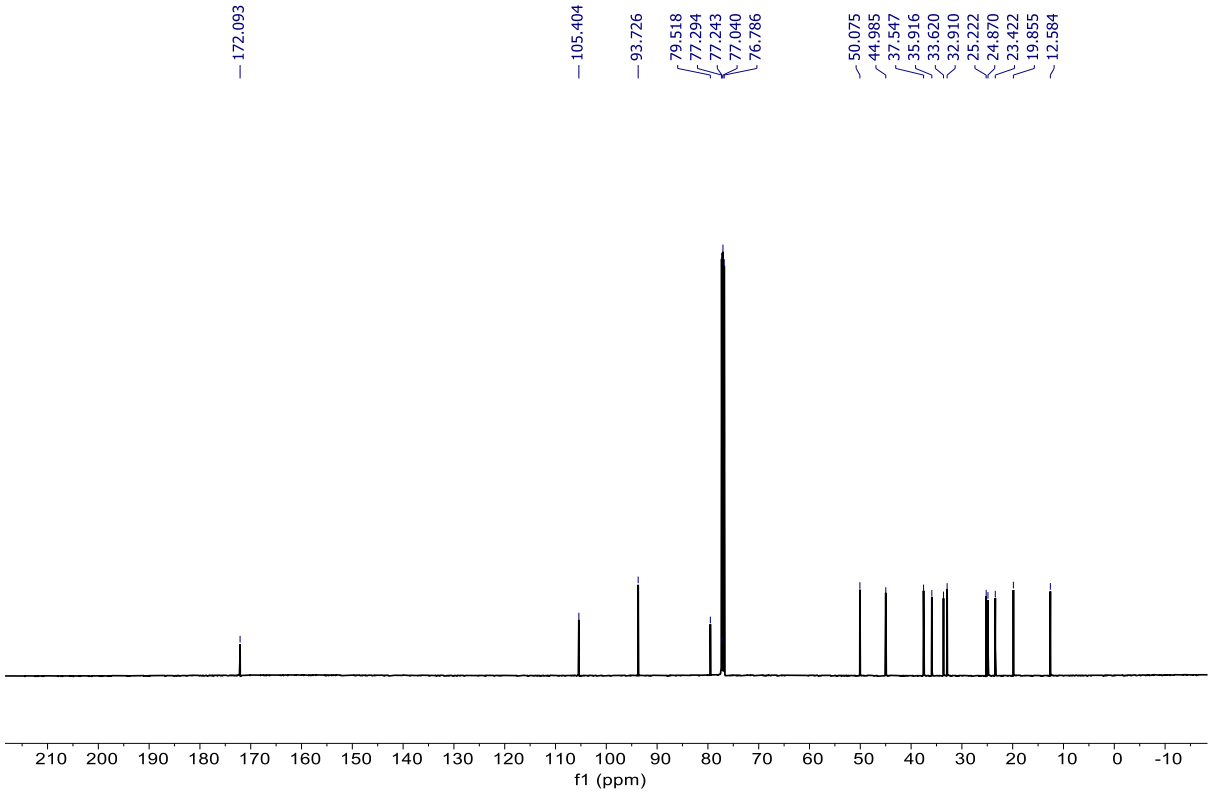

Figure S29 - ^{13}C NMR (125 MHz) of artemisinin in $CDCl_3$ at 298 K.

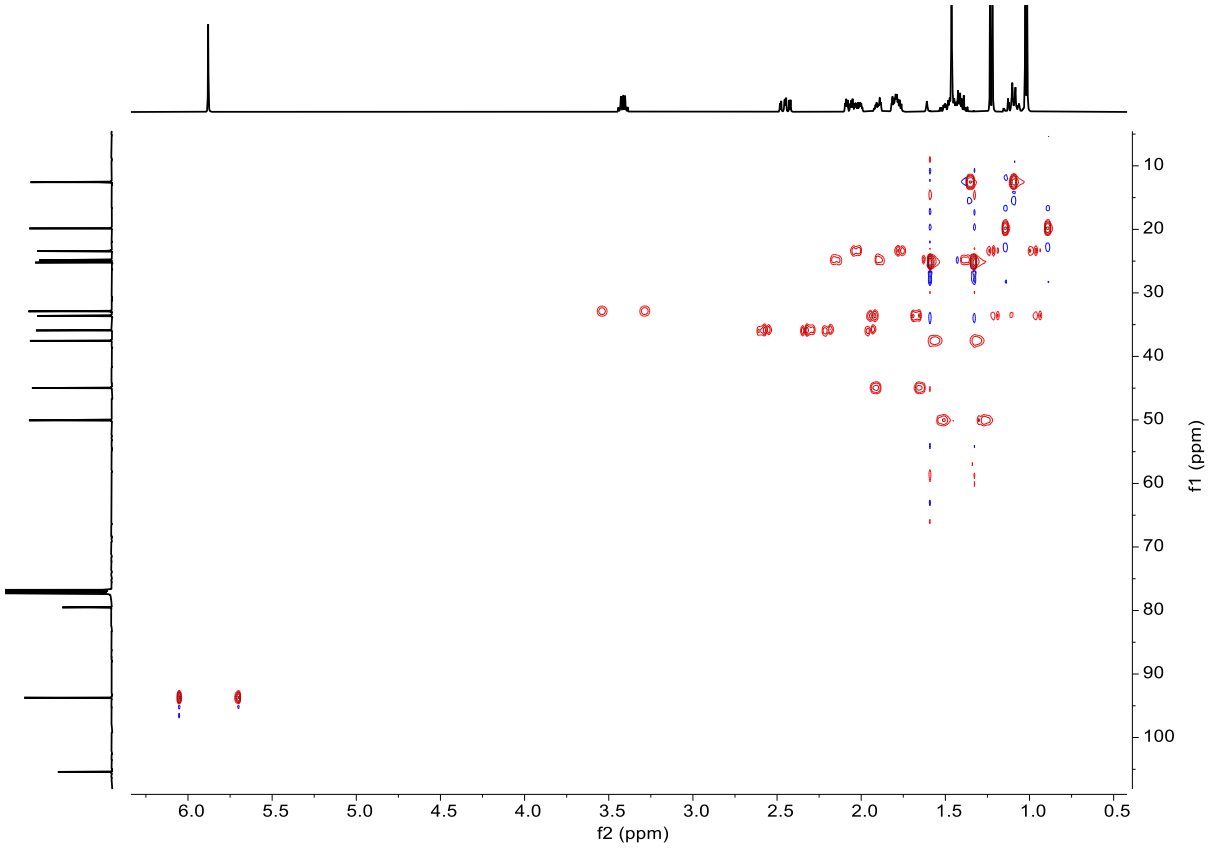

Figure S30 - [$^{1}H^{13}C$] CLIP-HSQC (500 MHz) of artemisinin in $CDCl_3$ at 298 K.

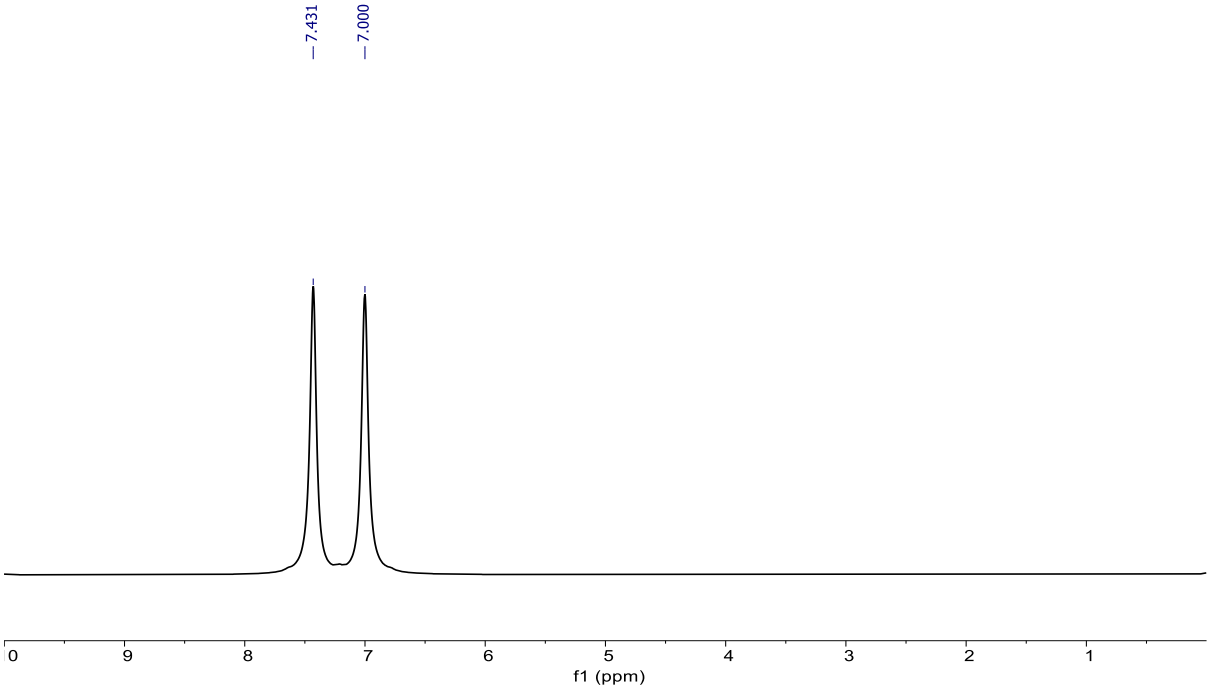

Figure S31 – ^{2}H NMR (75.6 MHz) of 15.7 mg/mL artemisinin and 18.1 mg/mL of GO-NP in $CDCl_3$ at 298 K after sonication.

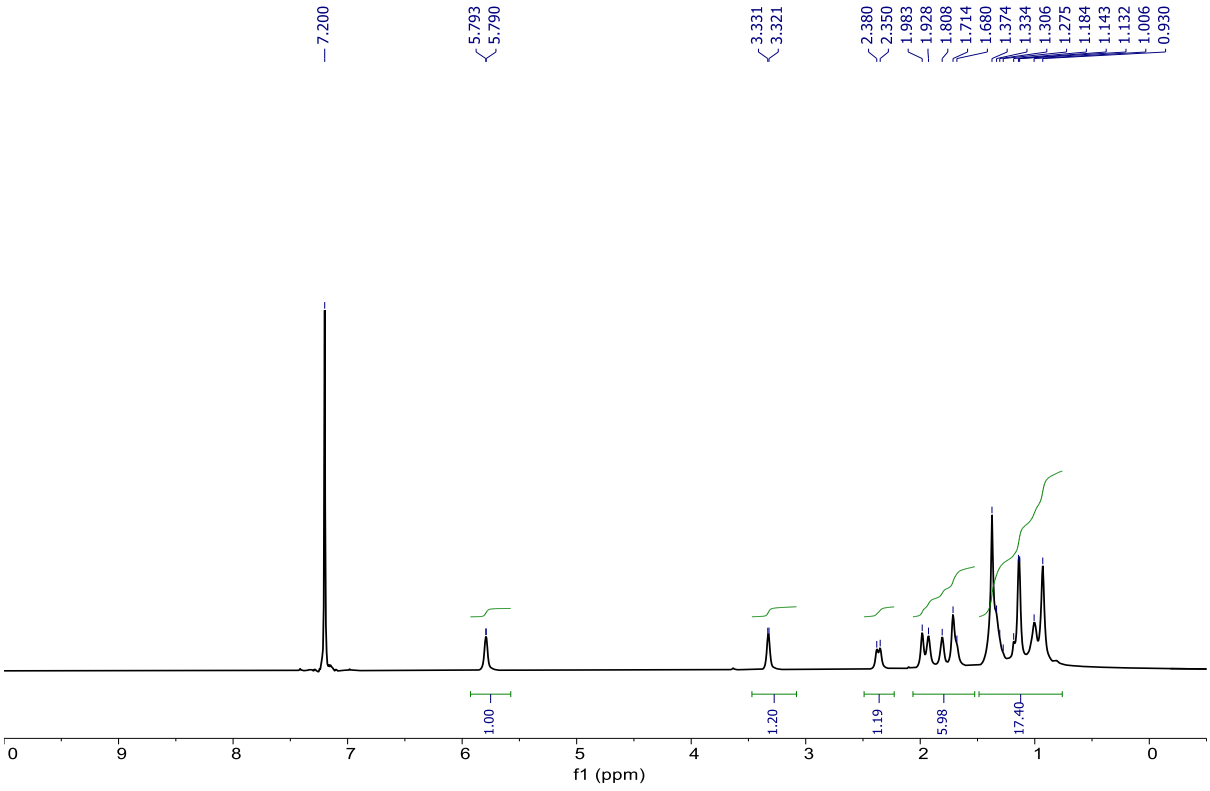

Figure S32 – ^{1}H NMR (75.6 MHz) of 15.7 mg/mL artemisinin and 18.1 mg/mL of GO-NP in $CDCl_3$ at 298 K after sonication.

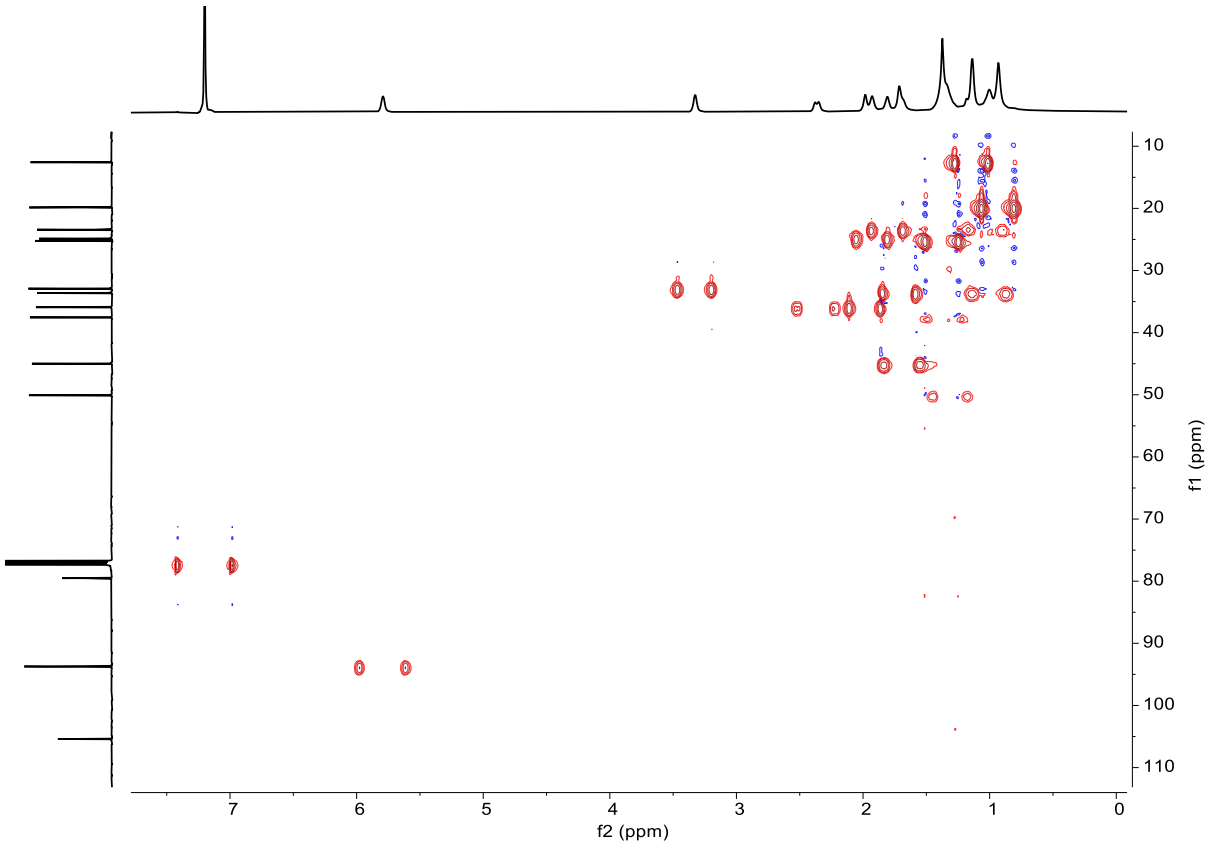

Figure S33 - [$^{1}H^{13}C$] CLIP-HSQC of artemisinin (500 MHz) in $CDCl_3$ at 298 K after sonication.

7.1. RDC of artemisinin

artemisinin		
Q = 0.13		
	Exp Hz	Comp Hz
C7,H26	9.25	10.86
C3,H25	17.9	19.2
C8,H27	16	13.18
C11,H32	17.9	19.12
C1,H21	-13.44	-13.83
C1,H22	40.85	39.29
C10,H30	3.2	1.71
C10,H31	6.9	7.11
C14,H33	16.62	16.93
C9,H28	22	22.93
C9,H29	-12.19	-11.62
C16,H34	2.28	1.4
C16,H35	2.28	1.4
C16,H36	2.28	1.4

Table S8 - Atom numbers and RDC values (experimental and calculated) for artemisinin.

7.2. SVD fitting of the artemisinin

Alignment tensor

A'x= 8.442e-05

A'y= 1.012e-03

A'z=-1.097e-03

Saupe tensor

S'x= 1.266e-04

S'y= 1.519e-03

S'z=-1.645e-03

Alignment tensor eigenvectors

e[x]=(-0.566,-0.429, 0.704)

e[y]=(0.818,-0.191, 0.542)

e[z]=(-0.099, 0.883, 0.459)

Alignment tensor in laboratory coordinates:

[6.944e-04,-4.205e-05,4.652e-04]

[-4.205e-05,-8.023e-04,-5.750e-04]

[4.652e-04,-5.750e-04,1.079e-04]

SVD condition number is 9.629e+00

Axial component Aa = -1.645e-03

Rhombic component Ar = -9.280e-04

rhombicity R = 0.564

Asimmetry parameter etha =8.461e-01

GDO = 2.214e-03

Euler Angles (degrees)

Set 1

(62.5,5.7,124.7)

Set 2

(-117.5,174.3,-55.3)

Grid points: 64

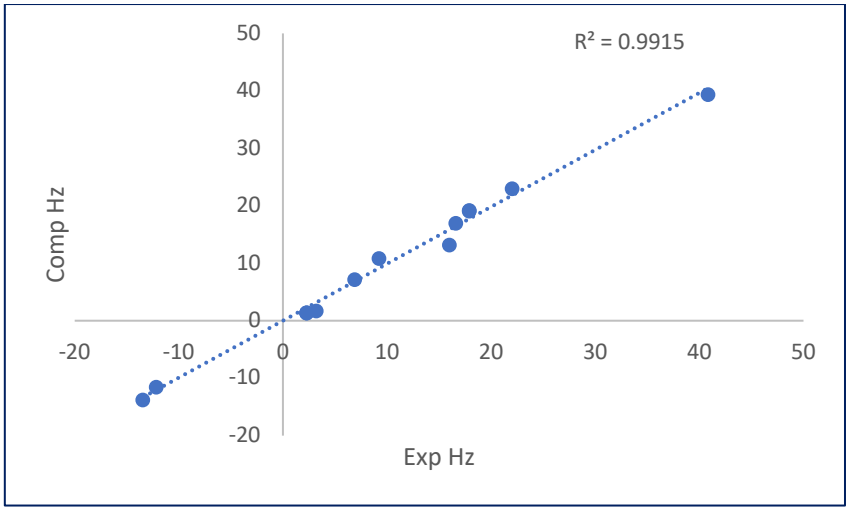

Figure S34 - Plot showing experimental versus calculated RDCs of artemisinin.

Diastereomers	Q
artemisinin	0.13
***6-epi*-artemisinin**	0.25
***6-9-epi*-artemisinin**	0.3

Table S9 - Q factors derived from RDC calculations for all possible diastereomers of artemisinin.

8. NMR data and structural calculations of strychnine

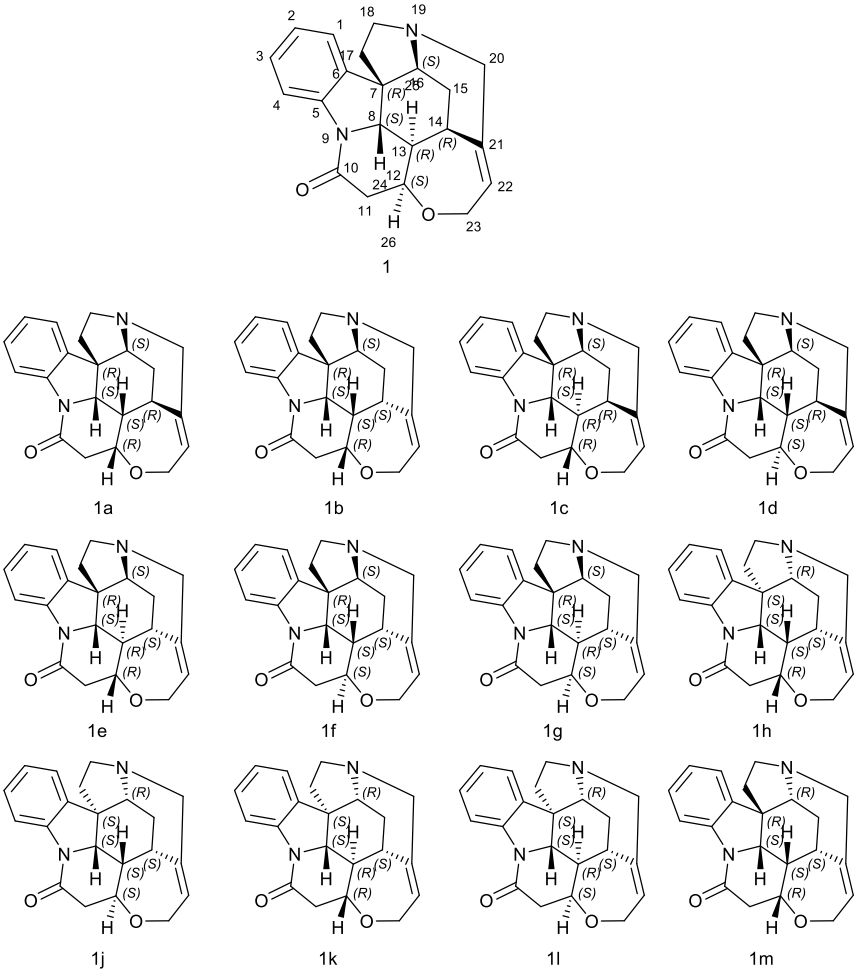

Figure S356 - Structures of all possible diastereomers of strychnine.

Atom numbering		
Chemdraw numbering	DFT numbering	^{13}C chemical shift assignment (ppm)
1	27	122.23
2	26	124.21
3	25	128.6
4	24	116.18
8	20	60.05
11a	3	42.43
11b	3	42.43
12	#4	77.57
13	18	48.13
14	#17	31.53
15a	16	26.75
15b	16	26.75
16	15	60.17
17a	13	42.78
17b	13	42.78
18a	12	50.35
18b	12	50.35
20a	10	52.66
20b	10	52.66
22	8	128.11
23a	7	64.56
23b	7	64.56
5		142.4
6		133
7		52.1
10		169.5
21		140.8

Table S10- Atom numbers and 13C chemical shift assignments of strychnine in $CDCl_3$.

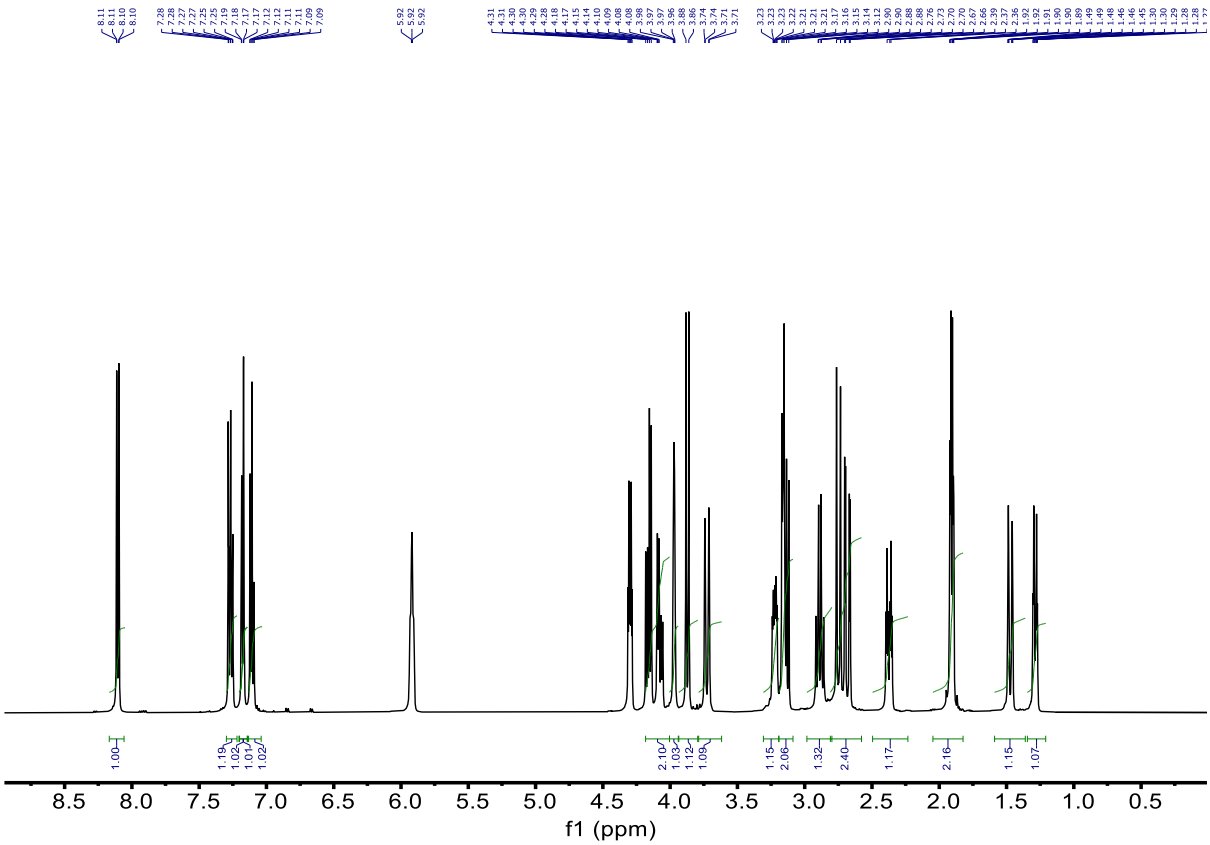

Figure S36 -^{1}H NMR (500 MHz) of strychnine in $CDCl_3$ at 298 K.

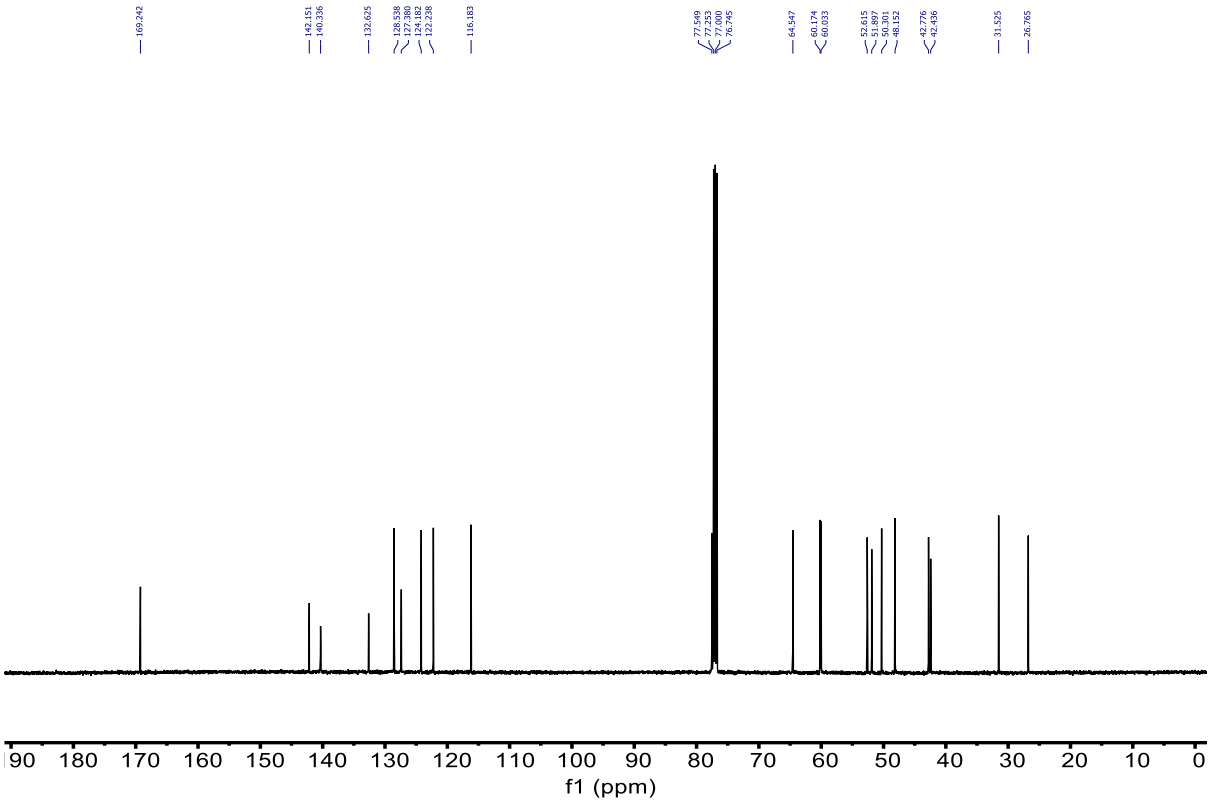

Figure S37 - ^{13}C NMR (500 MHz) of strychnine in $CDCl_3$ at 298 K.

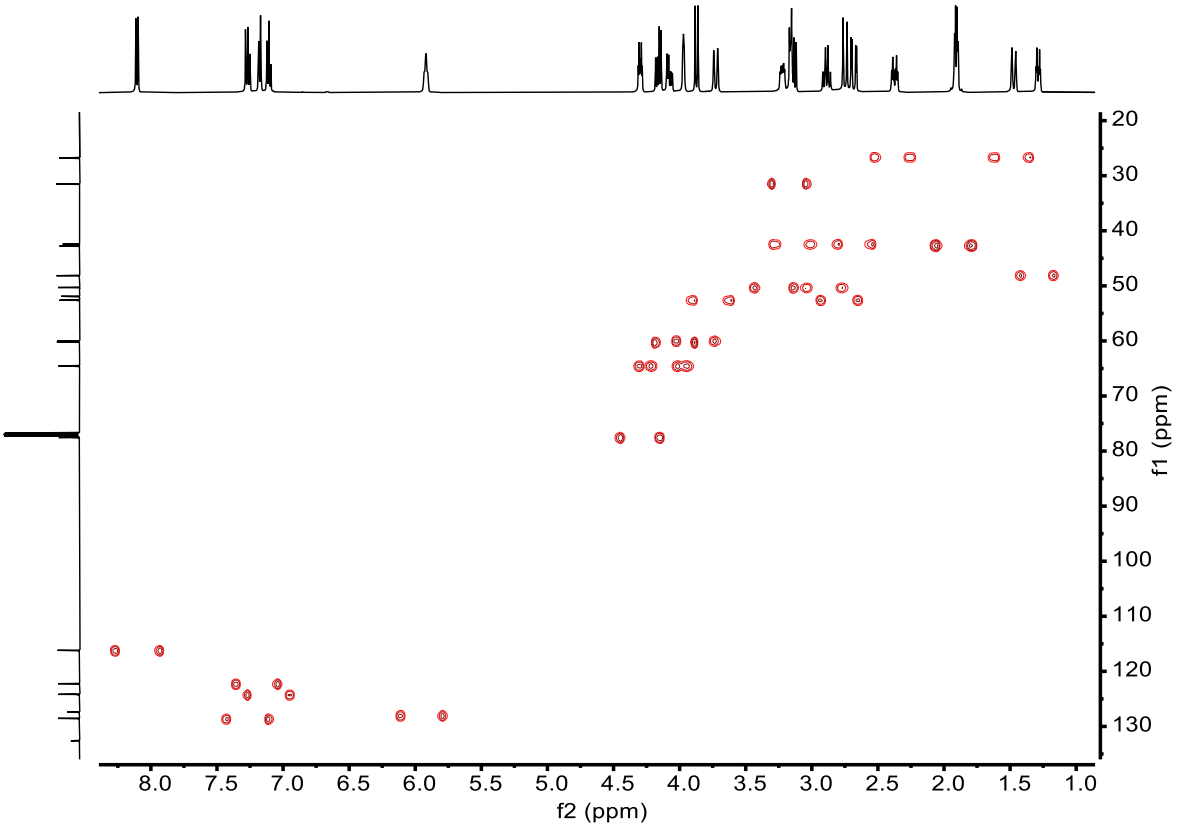

Figure S38 - [$^{1}H^{13}C$]-CLIP-HSQC (500 MHz) of strychnine in $CDCl_3$ at 298 K.

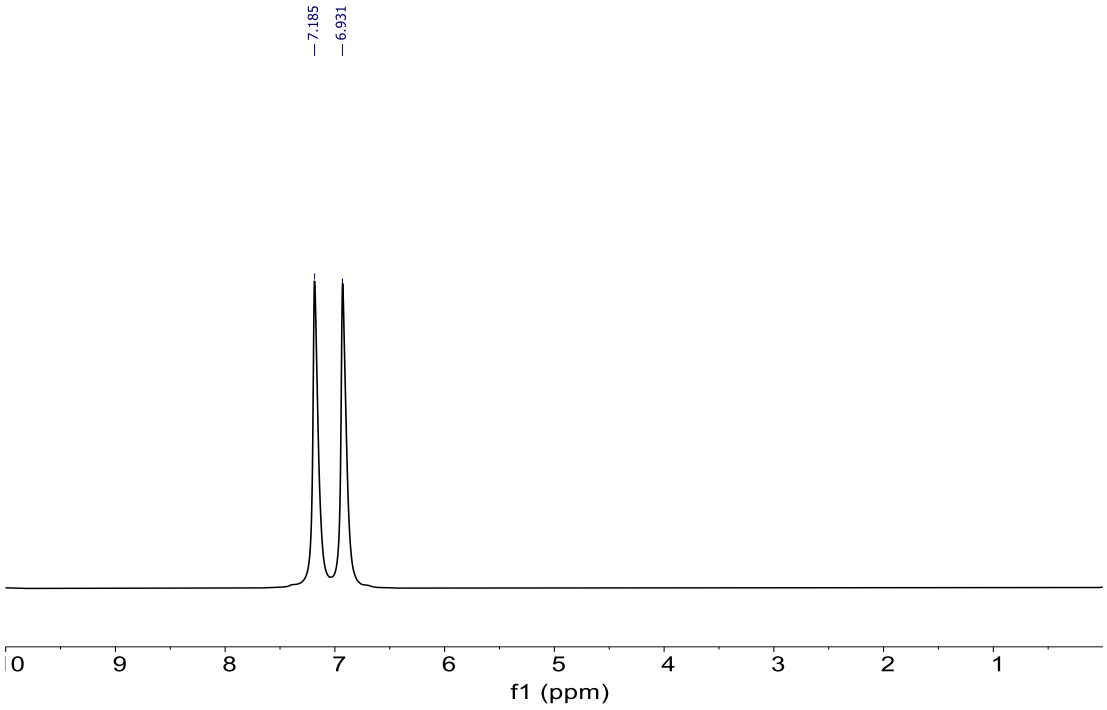

Figure S39 - ^{2}H NMR (75.6 MHz) of 14.4 mg/mL artemisinin and 14.9 mg/mL of GO-NP in $CDCl_3$ at 298 K after sonication.

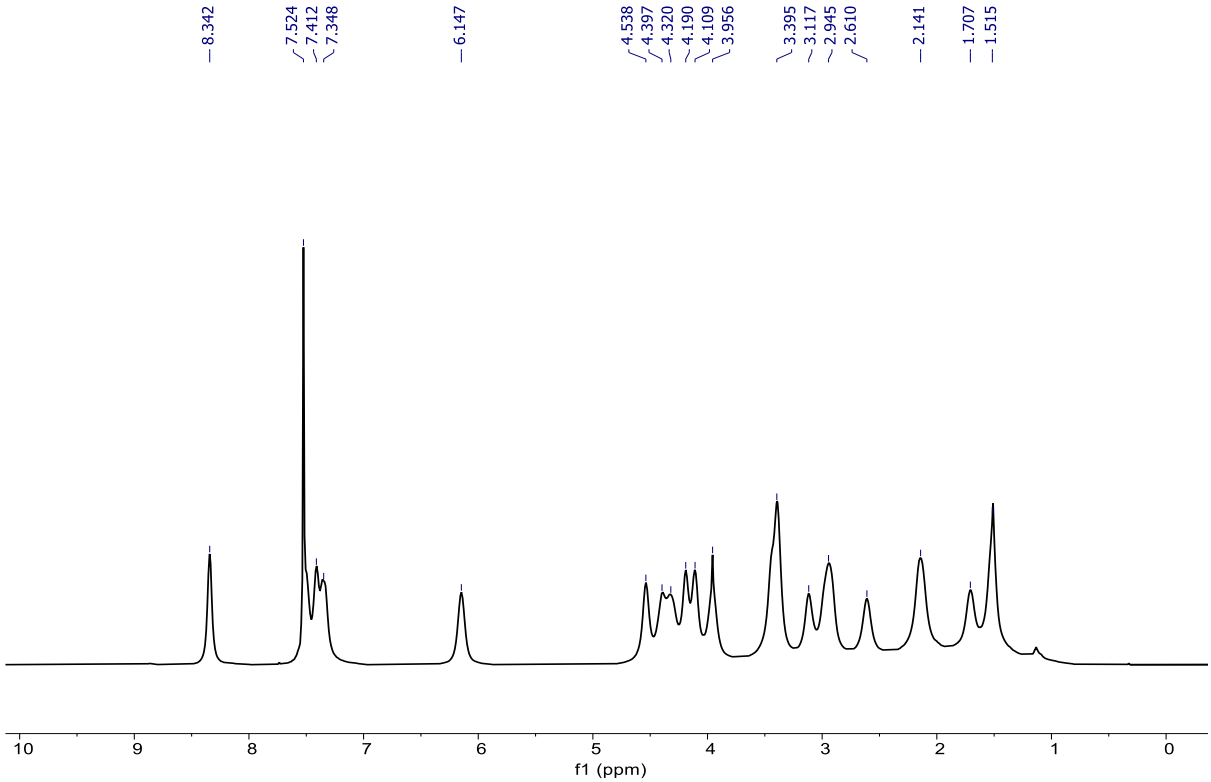

Figure S40 - ^{1}H NMR (500 MHz) of 14.4 mg/mL artemisinin and 14.9 mg/mL of GO-NP in $CDCl_3$ at 298 K after sonication.

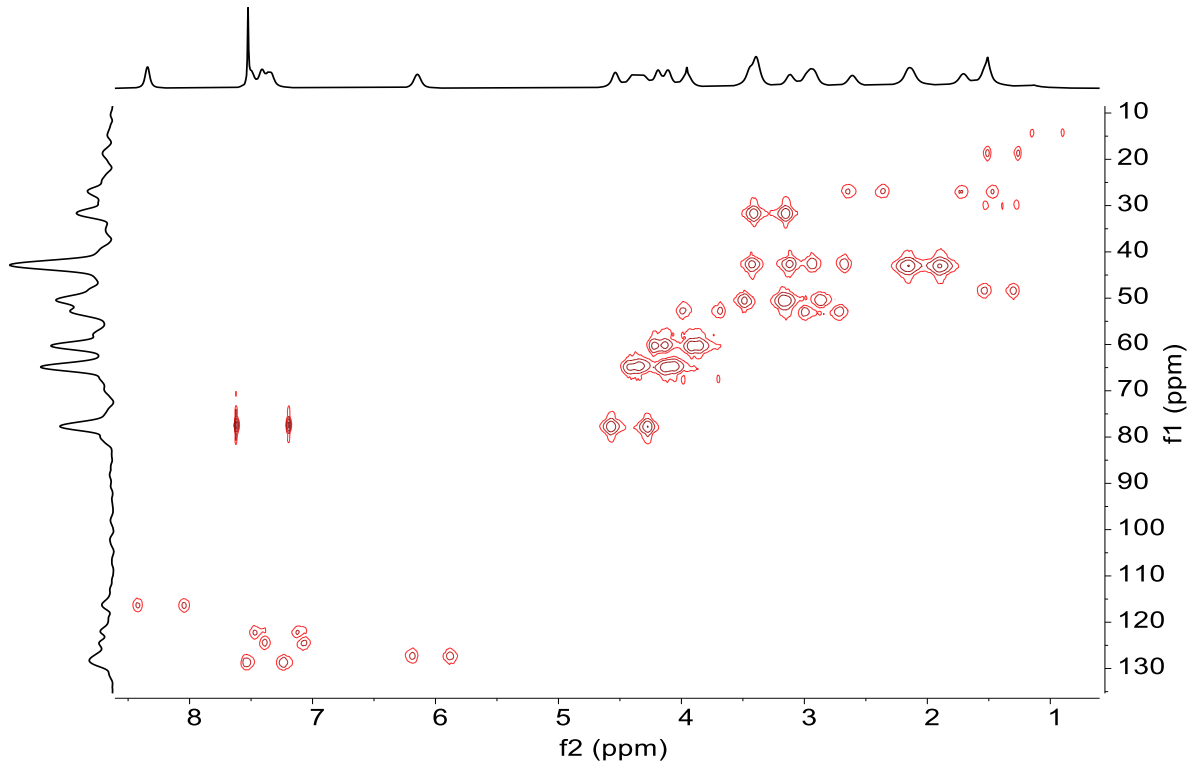

Figure S41 - [$^{1}H^{13}C$] CLIP-HSQC of 14.4 mg/mL artemisinin and 14.9 mg/mL of GO-NP in $CDCl_3$ at 298 K after sonication.

8.1. RDC of strychnine

RSSRRS diastereomer		
Q = 0.175		
	Exp Hz	Comp Hz
C24,H47	12.27	13.90
C22,H45	-8.31	-10.27
C21,H44	17.21	14.02
C18,H43	-1.53	-3.36
C4,H28	5.52	4.74
C17,H42	-5.20	-3.28
C16,H41	3.61	1.86
C15,H39	-2.63	-4.71
C15,H40	12.16	12.41
C12,H36	13.44	13.02
C12,H37	-9.70	-11.40

Table S11 - Atom numbers and 1DCH (experimental and calculated) RDCs for the RSSRRS diastereomer of strychnine.

8.2. SVD fitting of the strychnine

Alignment tensor

A'x=-1.266e-04

A'y=-2.078e-04

A'z= 3.344e-04

Saupe tensor

S'x=-1.899e-04

S'y=-3.117e-04

S'z= 5.016e-04

Alignment tensor eigenvectors

e[x]=(-0.869, 0.283, 0.405)

e[y]=(0.466, 0.200, 0.862)

e[z]=(0.163, 0.938,-0.306)

Alignment tensor in laboratory coordinates:

[-1.320e-04,6.288e-05,-5.560e-05]

[6.288e-05,2.759e-04,-1.461e-04]

[-5.560e-05,-1.461e-04,-1.439e-04]

SVD condition number is 2.962e+00

Axial component Aa = 5.016e-04

Rhombic component Ar = 8.125e-05

rhombicity R = 0.162

Asimmetry parameter etha =2.430e-01

GDO = 5.877e-04

Euler Angles (degrees)

Set 1

(108.0,-9.4,151.8)

Set 2

(-72.0,189.4,-28.2)

Grid points: 64

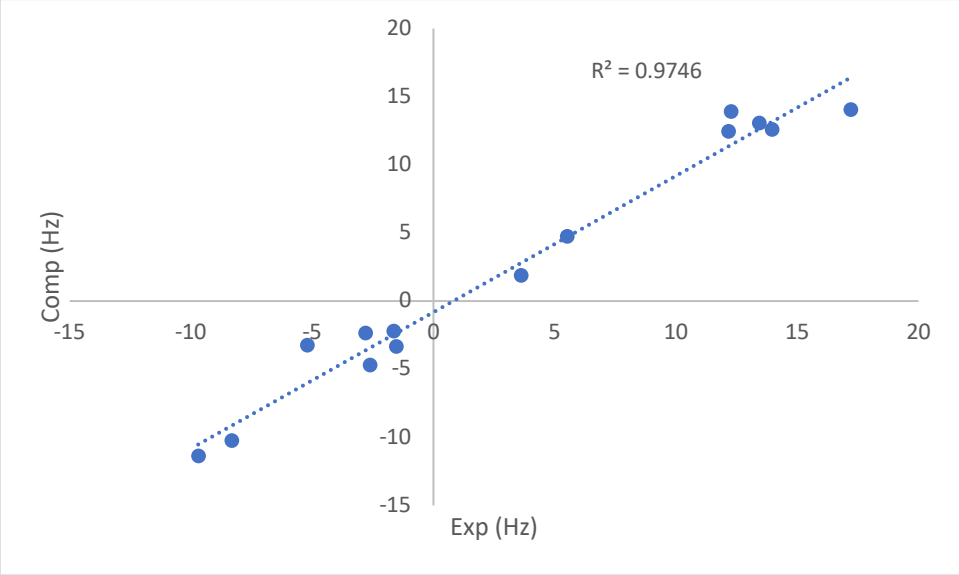

Figure S42 - Plot showing experimental versus calculated RDCs for the RSSRRS diastereomer of strychnine.

Diastereomers	Q
RSSRRS	0.175
RSSSSS	0.450
RSSRSS	0.450
RSSSRS	0.189
RSRRSS	0.264
RSSSRS	0.247
SRRSSS	0.395
RSSSRS	0.450
RSRRSS	0.395
RSRRSS	0.247

Table S12 - Q factors derived from RDC calculations for all possible diastereomers of strychnine.

9. ^{2}H NMR spectra of THF-d_8

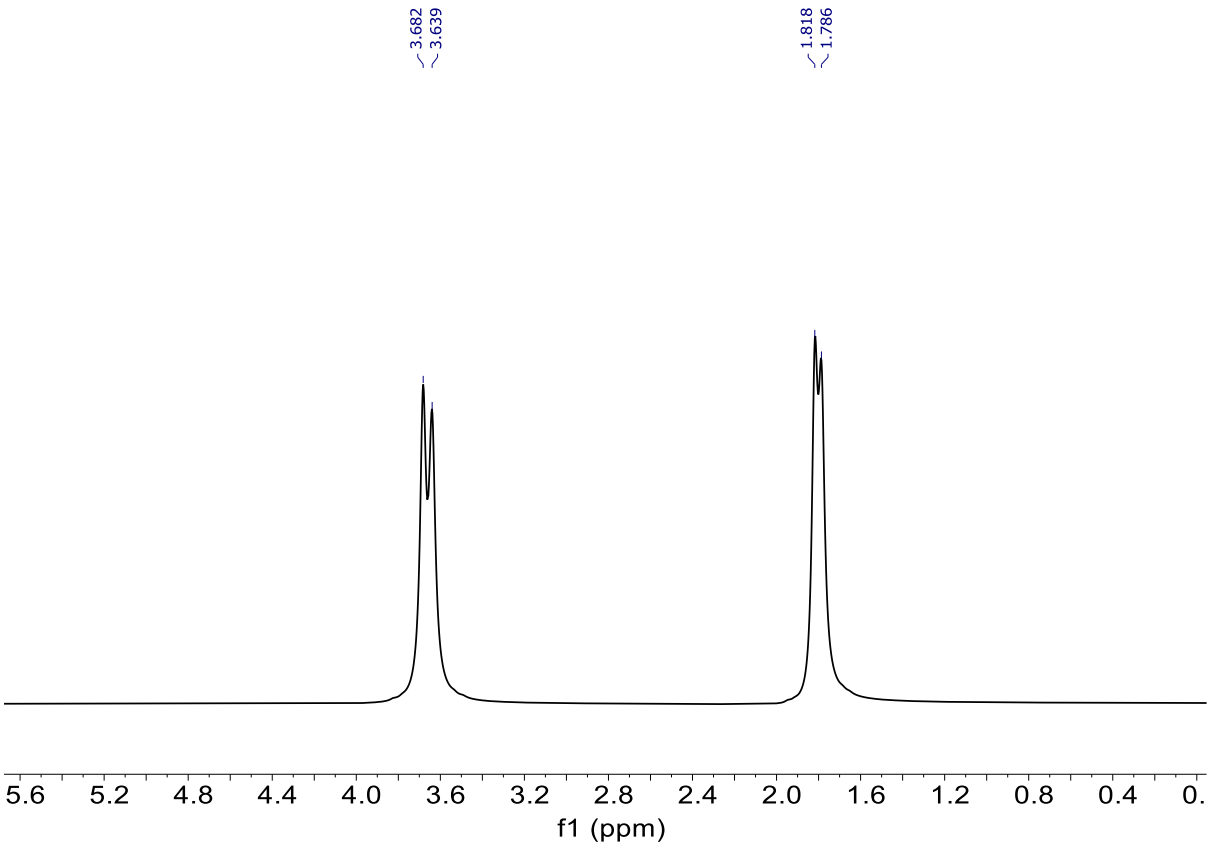

Figure S43 - ^{2}H NMR (75.6 MHz) of 12.2 mg/mL of GO-NP in THF-d_8.

10. References

1 F. Mohamadi, N. G. J. Richards, W. C. Guida, R. Liskamp, M. Lipton, C. Caufield, G. Chang, T. Hendrickson and W. C. Still, *J. Comput. Chem.*, 1990, **11**, 440–467.

2 A. D. Bochevarov, E. Harder, T. F. Hughes, J. R. Greenwood, D. A. Braden, D. M. Philipp, D. Rinaldo, M. D. Halls, J. Zhang and R. A. Friesner, *Int. J. Quantum Chem.*, 2013, **113**, 2110–2142.

3 K. S. Watts, P. Dalal, A. J. Tebben, D. L. Cheney and J. C. Shelley, *J. Chem. Inf. Model.*, 2014, **54**, 2680–2696.

4 Schrödinger Release 2025-3: Jaguar, Schrödinger, LLC, New York, NY, 2025.